

1 **Deep Learning, Explained:**  
2 **Fundamentals, Explainability, and Bridgeability to Process-based Modelling**

3 Saman Razavi

4 Associate Professor, Global Institute for Water Security, School of Environment and Sustainability,  
5 University of Saskatchewan, Department of Civil, Geological and Environmental Engineering, Canada  
6 [saman.razavi@usask.ca](mailto:saman.razavi@usask.ca)

7 **Abstract**

8 Recent breakthroughs in artificial intelligence (AI), and particularly in deep learning (DL), have created  
9 tremendous excitement and opportunities in the earth and environmental sciences communities. To  
10 leverage these new ‘data-driven’ technologies, however, one needs to understand the fundamental  
11 concepts that give rise to DL and how they differ from ‘process-based’, mechanistic modelling. This paper  
12 revisits those fundamentals and addresses 10 questions often posed by earth and environmental  
13 scientists with the aid of a real-world modelling experiment. The overarching objective is to contribute to  
14 a future of AI-assisted earth and environmental sciences where DL models can (1) embrace the typically  
15 ignored knowledge base available, (2) function credibly in ‘true’ out-of-sample prediction, and (3) handle  
16 non-stationarity in earth and environmental systems. Comparing and contrasting earth and  
17 environmental problems with prominent AI applications, such as playing chess and trading in stock  
18 markets, provides critical insights for better directing future research in this field.

19 **Plain Language Summary**

20 Deep learning (DL) is an artificial intelligence (AI) technique that has already served the vast majority, if  
21 not all, of everyday society in tasks such as image recognition and language processing through  
22 smartphones. The recent unprecedented performance of DL in those tasks has accelerated applications  
23 in non-native areas such as earth and environmental sciences where knowledge-based modelling has  
24 dominated to date. A major challenge, however, is DL and knowledge-based modelling are rooted in  
25 different worldviews towards problem solving. This paper explains the ‘whats’ and ‘whys’ of DL from first  
26 principles, with an eye on applications since inception in environmental problems. An experiment is run  
27 to illustrate the fundamental differences between the two worldviews, and to shed light on some critical,  
28 but often ignored, issues DL may face in practice, largely arising from the fact that earth and  
29 environmental systems are complex with behaviors changing in ways that are physically explainable but  
30 not seen in the period of record due to uncertain factors such as climate change. Such issues must be  
31 addressed at the heart of the endeavor to develop DL techniques that embrace the knowledge base  
32 available, in anticipation of breakthroughs in an age of big data and computational power.

33 **Keywords**

34 Artificial intelligence, machine learning, deep learning, artificial neural networks, process-based  
35 modelling, earth systems, hydrology

36

37 **Key Points**

- 38 • DL is rooted in *connectionism*, *hyper-flexibility*, and *vigorous optimization*, which are alien to  
39 conventional knowledge-based modelling.
- 40 • A knowledge base is essential to enable credible predictions of *complex*, *open*, *partially observable*,  
41 and *non-stationary systems*.
- 42 • Bridging DL and earth and environmental sciences is still embryonic but has great potential in an age  
43 of big data and computational power.

44 **Table of Contents**

45 1. The rise of deep learning ..... 3

46 2. Back to fundamentals ..... 4

47 2.1. Why ML and DL? ..... 4

48 2.2. Evolution of DL and major milestones ..... 5

49 2.3. Latest developments and rebranding the field ..... 8

50 3. Geometrical Interpretation of DL ..... 9

51 3.1. A perceptron ..... 10

52 3.2. ANNs with one hidden layer ..... 11

53 3.3. So, why more than one hidden layer? ..... 13

54 4. Relevance of Occam’s razor and equifinality? ..... 14

55 4.1. Issues with the complexity of ANNs ..... 14

56 4.2. Leashing the hyper-flexibility of ANNs ..... 15

57 5. Fundamental differences from other ML methods ..... 17

58 5.1. Local versus distributed representations ..... 17

59 5.2. Implications for users ..... 18

60 6. How to introduce order, time-dependency, and memory ..... 19

61 6.1. Tapped delay lines ..... 19

62 6.2. Recurrent connections ..... 20

63 6.3. Gate layers to forget or preserve over time ..... 21

64 6.4. Training considerations when the order of data matters ..... 21

65 7. ML versus process-based modelling – An experiment ..... 22

66 7.1. Data and models ..... 22

67 7.2. Model performance in calibration ..... 24

68 7.3. What about *a priori* information encoded in models? ..... 25

69 7.4. Model validation: Standard versus true out-of-sample prediction ..... 25

70 7.5. Injecting some physics into ML ..... 27

71 7.6. So, what model should we trust: the ML or process-based model? ..... 28

72 8. Discussion ..... 29

73 8.1. What is the typically ignored value of domain knowledge in DL? ..... 29

74 8.2. Why is DL essentially different from process-based modelling? ..... 30

75 8.3. How can we bridge DL and process-based modelling? ..... 31

76 8.4. What can we learn from prominent DL applications? ..... 33

77 9. Concluding remarks ..... 34

78 References ..... 35

79

## 80 1. The rise of deep learning

81 The last decade has witnessed a tremendous rise in techniques called ‘deep learning’ (DL), under the  
82 umbrella of artificial intelligence (AI) and machine learning (ML), and their unprecedented performance  
83 in areas such as computer vision (Krizhevsky et al., 2017), natural language processing (Young et al., 2018),  
84 and gaming (Silver et al., 2018). These successes have motivated the application of DL across a wide range  
85 of disciplines, including medicine (Hosny et al., 2018), earth sciences (Reichstein et al., 2019), robotics  
86 (Torresen, 2018), engineering (Panchal et al., 2019), and finance (Lee et al., 2019). DL owes its exemplary  
87 success to the boom in computational power and the emergence of big data sources and associated data  
88 storage and sharing technologies.

89 Earth and environmental sciences appear to be positioned to benefit profoundly from DL, as big data  
90 sources on a range of *in situ* and remotely-sensed variables are becoming increasingly available with the  
91 advances in sensing technologies (Reichstein et al., 2019). The storage volume of remote sensing data for  
92 earth observations is already well beyond dozens of petabytes, with transmission rates exceeding  
93 hundreds of terabytes per day. Datasets based on model outputs are rising; for example, the climate  
94 assessment dataset provided by the Coupled Model Intercomparison Project Phase 6 may reach 40  
95 petabytes (Eyring et al., 2016). Reanalysis climatic datasets have also grown; for example, NASA’s Modern-  
96 Era Retrospective Analysis for Research and Applications version 2 (MERRA-2) is ~400 terabytes (Gelaro  
97 et al., 2017). In addition, datasets generated via tens of thousands of citizen science projects are providing  
98 large and rich sources of ground-based data.

99 This potential is shifting the attention of earth and environmental scientists and relevant funding agencies  
100 towards ML, as evidenced, for example, by the shift in research work presented at the American  
101 Geophysical Union (AGU)’s fall meetings, the largest assembly of earth and environmental scientists with  
102 more than 27,000 people in attendance and 25,000 presentations in 2019. The number of ML-related  
103 presentations has risen consistently—from 0.2% of total presentations in 2015 to 4.2% in 2020. In  
104 particular, this shift has been astonishing in the ‘non-linear geophysics’, ‘earth and space science  
105 informatics’, ‘natural hazards’, ‘hydrology’, and ‘seismology’ sub-fields, where 28 (2.1), 18 (5.1), 9 (1.3),  
106 7.5 (1.4), and 6.7% (0.9%) of total presentations, respectively, were related to ML in 2020 (2015).

107 Recent successful applications of DL techniques to earth and environmental sciences include weather  
108 nowcasting and forecasting (Shi et al., 2015; Shi et al., 2017), satellite precipitation bias reduction (Tao et  
109 al., 2006), rainfall-runoff modelling (Kratzert et al., 2018; Feng et al., 2020; Ma et al., 2021), rain and snow  
110 retrieval from spaceborne sensors (Tang et al., 2018), downscaling hydroclimatic variables (Ducournau  
111 and Fablet, 2016), precipitation estimation (Tao et al., 2018; Pan et al., 2019), and surrogate modelling  
112 (Gu, et al., 2020; Yu et al., 2020; Vali et al., 2021). Unsuccessful applications, perhaps similar to many other  
113 areas, remain largely unreported in the peer-reviewed scientific literature but occasionally appear in other  
114 media (e.g., Wexler, 2017; Kolakowski, 2018; Rudin, 2019).

115 Notably, most DL algorithms, formerly known as artificial neural networks (ANNs), have been around and  
116 widely applied in earth and environmental sciences since the early 1990s with the birth of domains such  
117 as Hydroinformatics (Abbott, 1991). These applications are documented in reviews by Gardner and  
118 Dorling (1998), Maier and Dandy (2000), Krasnopolsky (2007), Maier et al. (2010), Abraham et al. (2012),  
119 Razavi et al. (2012a), Shen (2018), Bergen et al. (2019), and Reichstein et al. (2019). Arguably, however,

120 the uptake of DL to facilitate and advance earth and environmental sciences has not kept pace with data  
121 availability and computational power over the past three decades.

122 But why? The challenges impeding the widespread application of DL to earth and environmental problems  
123 to date may be rooted in the fact that convincingly casting those problems, for which an extensive  
124 knowledge base is usually available, within the DL framework is often not straightforward. Moreover, the  
125 lack of interpretability and explainability of DL has been a major hindrance, as model developers need to  
126 be able to make sense of why a model functions the way it does, and to explain that to model users. These  
127 challenges can be further complicated in the absence of a solid understanding of the fundamentals of DL  
128 and how they differ from theory-driven, mechanistic modelling and prediction. Mechanistic modelling,  
129 also called process-based or knowledge-based modelling in this paper, has traditionally been the  
130 cornerstone of scientific advancement and policy support.

131 And why this paper? Motivated by the recent breakthroughs by DL in its original areas of application,  
132 namely computer vision and natural language processing, this paper aims to address the persistent  
133 challenges facing DL applications in non-native areas related to earth and environmental sciences. With  
134 this overarching aim, this paper addresses 10 questions regarding the fundamentals of DL and its  
135 explainability and bridgeability to earth and environmental systems modelling:

- 136 (1) What is DL and how did it evolve from ANNs?
- 137 (2) How can we interpret the internal functioning of DL?
- 138 (3) How can the complexity of DL be justified in light of the principle of parsimony?
- 139 (4) Why is DL considered superior to other types of ML?
- 140 (5) How can DL account for memory and time dependency?
- 141 (6) How may DL and process-based models behave differently in out-of-sample prediction?
- 142 (7) What can be the often ignored value of domain knowledge in DL?
- 143 (8) Why is DL essentially different from process-based modelling?
- 144 (9) What are the existing approaches to bridging DL and process-based modelling?
- 145 (10) What can we learn from prominent DL applications such as gaming and the stock market?

146 The structure of this paper is such that it best serves the reader when all sections are followed  
147 sequentially. However, an advanced reader could directly refer to a section designated to address a  
148 question of interest. Sections 2 through 7 address questions 1 through 6 and sub-sections 8.1 through 8.4  
149 address questions 7 through 10, respectively. A real-world hydrological modelling problem and multiple  
150 synthetic functions are used to explain complex concepts via simple examples. The contents of this paper  
151 are intended to be accessible to a wide audience from various fields under the umbrella of earth and  
152 environmental sciences. However, the views presented mainly arise from the author's data- and theory-  
153 driven research background in hydrology and water resources.

## 154 **2. Back to fundamentals**

### 155 **2.1. Why ML and DL?**

156 ML, and in particular DL, is nowadays concerned with developing machines that improve their own  
157 performance in carrying out a given task over time by 'learning' from examples, with minimal human  
158 efforts to instruct the machines how to do so (Jordan and Mitchell, 2015). According to Goodfellow et al.  
159 (2016), however, the early efforts to generate AI were based on a knowledge base paradigm to instruct

160 machines with a formal set of step-by-step mathematical and if-then rules. Those efforts focused on  
161 carrying out tasks that were intellectually difficult for humans but straightforward for computers.  
162 [Goodfellow et al. \(2016\)](#) argue such efforts led to no major successes, and the AI of today is about enabling  
163 machines to perform tasks that humans perform intuitively and rather easily but have difficulty formally  
164 describing how they do so. Examples of such tasks include recognizing faces in a photo or comprehending  
165 spoken words.

166 Not only did state-of-the-art AI divorce from the knowledge base, but it also completely separated from  
167 classic data-driven modelling rooted in statistics such as regression. This separation was a response to the  
168 need for models that are not constrained by the many assumptions typical statistical models hold. For  
169 example, traditional statistical modelling requires a formalization of relationships between variables and  
170 assumptions about functional shapes, distributions of variables, and their inter-dependencies, which  
171 enables hypothesis testing and the generation of confidence bounds. Conversely, in the ML context the  
172 underlying relationships in data may have any complex form, which is typically unknown *a priori*, and the  
173 data used may have any size and distributional properties (see [Dangeti, 2017, p. 10-11](#)).

174 Because of these characteristics, ML is deemed suitable to pursue the longstanding ambition to build  
175 machines that work with minimal or no human supervision and imposed assumptions. As a result, ML  
176 techniques nowadays, and in particular DL, provide flexible tools that can adapt to a wide range of data  
177 and applications.

## 178 **2.2. Evolution of DL and major milestones**

179 It was 1957 when Frank Rosenblatt invented the first algorithm, termed ‘perceptron’ ([Rosenblatt, 1957](#)),  
180 which today forms the smallest computational unit of DL. A perceptron, alternatively termed a ‘neuron’  
181 because of its resemblance to the basic working unit of the brain, is shown in [Figure 1a](#) and formulated  
182 as:

$$183 \quad y = f\left(\sum_{i=1}^D w_i x_i + b\right) \quad (\text{Eq. 1})$$

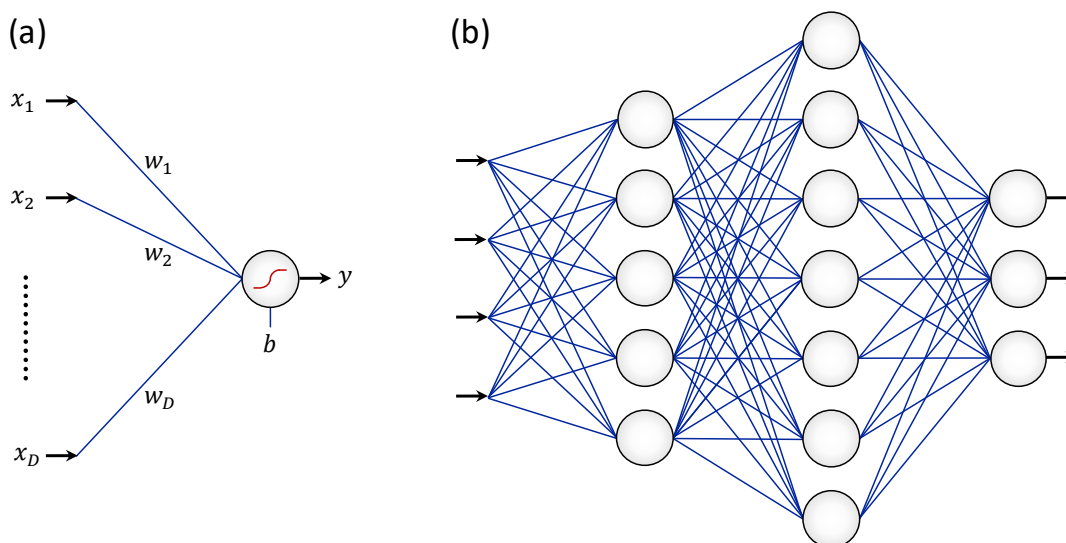
184 where  $D$  is the dimension of input space,  $\mathbf{x}$  is the input vector,  $\mathbf{w}$  is a set of weights corresponding to the  
185 input vector,  $b$  is bias, and  $f$  is an ‘activation’ function. A perceptron has  $D+1$  tunable parameters (i.e.,  $D$   
186 weights and one bias) and is basically nothing but a multiple linear regression augmented by an output  
187 function ( $f$ ), which is non-linear. The form of the activation function was originally a step function, but  
188 now a range of monotonic functional forms, such as ‘sigmoidal’, are used.

189 The invention of perceptrons created significant excitement in the AI community and beyond. But, it soon  
190 became clear that a perceptron would not be able to map input spaces that are not linearly separable,  
191 such as the XOR problem ([Minsky and Papert, 1969](#)), rendering perceptrons of limited use in real-world  
192 applications. The reason for this inability is that the core of the perceptron is a linear regression.

193 Efforts to overcome this barrier could have followed two different avenues. Perhaps the most intuitive  
194 avenue was to employ non-linear regression, by allowing the terms inside the parentheses in Eq. 1 to be  
195 of other algebraic forms such as quadratic. However, this was not a viable option in part because the user  
196 then would need to specify the form of non-linearity which is not typically known *a priori*, requiring  
197 possibly extensive trial-and-error.

198 The second avenue that led to today's DL was to combine perceptrons both in parallel and in series to  
 199 create so-called 'multi-layer perceptrons' (MLPs), as shown in **Figure 1b**, with the hope this more complex  
 200 system could overcome the barrier. An MLP would then have many more tunable parameters than the  
 201 perceptron. The first layer, also called the first 'hidden' layer, would have  $D \cdot n_1$  weights and  $n_1$  biases,  
 202 where  $n_1$  is the number of neurons in this layer. Similarly, the second hidden layer would have  $n_1 \cdot n_2$   
 203 weights and  $n_2$  biases, and the last layer, called the 'output' layer would have  $n_{d-1} \cdot n_d$  weights,  
 204 where  $n_{d-1}$  and  $n_d$  are the numbers of neurons in the second-to-last and last layers, respectively, and  $d$  is  
 205 the total number of layers. The total number of layers in an MLP and the number of neurons in each layer  
 206 are 'hyper-parameters', to be specified by users. Also important is the choice of activation functions in  
 207 each layer. Note that a linear activation function is typically only suitable for the last layer and, in general,  
 208 any stack of linear layers is effectively equivalent to a single linear layer.

209 MLPs are a prominent class of 'artificial neural networks' (ANNs), or simply 'neural networks' (NNs), a  
 210 name reflecting their perceived resemblance to biological neural networks. MLPs, which are sometimes  
 211 called 'feedforward neural networks' (FNNs), are the building blocks of a range of other ANNs developed  
 212 later on, including 'autoencoders' (Bourlard and Kamp, 1988), 'recurrent neural networks' (RNNs; Elman,  
 213 1990) and its popular variation 'long short-term memory' (LSTM; Hochreiter and Schmidhuber, 1997),  
 214 convolutional neural networks (CNNs; Lawrence et al., 1997), and generative adversarial networks (GANs;  
 215 Goodfellow et al., 2014).



216  
 217 **Figure 1.** (a) A perceptron and (b) a multi-layer perceptron with four inputs, two hidden layers, and  
 218 three outputs.

219  
 220 But, MLPs on their own did not go far and the field stagnated for many years because of the absence of  
 221 an algorithm that could automatically derive from data the network weights and biases—a process  
 222 referred to as 'training' in the AI community. It took until the mid-1980s when the first 'back-propagation'  
 223 (BP) algorithm was invented to enable the training of MLPs with any network structure (Rumelhart et al.,  
 224 1986). This invention marked the beginning of the 'second wave' of popularity of ANNs. BP is essentially

225 an optimization algorithm, based on non-linear programming, that minimizes a loss function representing  
226 the goodness-of-fit of predictions to observations, such as the ‘sum of squared errors’, as follows:

$$227 \quad F = \sum_{k=1}^M \sum_{j=1}^N (T_j^k - y_j^k)^2 \quad (\text{Eq. 2})$$

228 where  $y_j^k$  is the output of neuron  $j$  in the output layer when the network is forced with input data sample  
229  $k$  and  $T_j^k$  is the respective desired target. Also,  $M$  is the size of training data, and  $N$  is the number of  
230 neurons in the output layer.

231 Different variations of BP rooted in first- (e.g., gradient descent) or second-order (e.g., Newton's method)  
232 optimization, or a combination thereof, now exist; see e.g., the Levenberg-Marquardt algorithm as  
233 implemented by Hagan and Menhaj (1994). These algorithms are fundamentally the same as optimization  
234 algorithms used nowadays for calibration of process-based models. The only difference is that, in the case  
235 of ANNs, and unlike most process-based models, the partial derivatives of the loss function with respect  
236 to weights and biases are *analytically* available and obtained through the ‘chain rule of differentiation’.  
237 More recently, derivative-free and metaheuristic optimization algorithms have shown promise in ANN  
238 training (e.g., Dengiz et al., 2009; Rakitianskaia and Engelbrecht, 2009; Razavi and Tolson, 2011), but have  
239 yet to become mainstream.

240 The training of ANNs is an iterative optimization process, where the network parameters are updated  
241 after each iteration (called an ‘epoch’ in the ANN context), to minimize the loss function. This process can  
242 be via ‘batch training’, where at each epoch the entire batch of training data (i.e., all  $M$  input-output sets)  
243 are used. Alternatively, each epoch can follow ‘mini-batch training’ based on a subset of training or  
244 ‘incremental/online training’ based on a single training data sample, chosen randomly or otherwise  
245 (Hagan et al., 1996). These two approaches, also commonly referred to as ‘stochastic gradient descent,  
246 are useful when the size of training data is large (Bottou, 1998; Bottou, 2010).

247 In the late 1980s, after the invention of BP, MLPs were proven to be ‘universal approximators’ (Hornik et  
248 al., 1989). This proof indicated MLPs with only one single-hidden layer that possesses a sigmoidal  
249 activation function, and a linear output layer, would be able to approximate any function with any desired  
250 level of accuracy provided the number of hidden neurons is sufficient. Since then, the ‘universal function  
251 approximation theorem’ has been the fundamental driver of interest in MLPs across a variety of disciplines  
252 and applications.

253 ANNs started receiving much attention in earth and environmental sciences in the early 1990s. The  
254 pioneering applications of ANNs include: Benediktsson et al. (1990), Badran et al. (1991), Stogryn et al.  
255 (1994), Bankert (1994), and Cabrera-Mercader and Staelin (1995) in the context of remote sensing of the  
256 environment; McCann (1992), Boznar et al. (1993), and Navone and Ceccatto (1994) in the context of  
257 atmospheric forecasting; and Kang et al. (1993), Hsu et al. (1995), and Minns and Hall (1996) in the context  
258 of hydrology modelling. Perhaps the most prominent and widely used application of ANNs in these fields  
259 has been related to the development of PERSIANN, or ‘Precipitation Estimation from Remotely Sensed  
260 Information using Artificial Neural Networks’ (Hsu et al., 1997; Sorooshian et al., 2000; Ashouri et al.,  
261 2015), which has been maintained and updated for two decades (accessible at  
262 <https://chrdata.eng.uci.edu/>).

263 Despite all of these advances, investments in ANNs and therefore the popularity of ANNs saw a decline in  
264 the AI community beginning in the mid-1990s. This was perhaps triggered by failures to fulfill overly

265 ambitious or unrealistic promises by prominent AI scientists (Goodfellow et al., 2016) that brought about  
266 somewhat a negative reputation for ANNs (Duerr et al., 2020), as historically observed in ‘AI winters’  
267 (Hendler, 2008). ANNs in earth and environmental sciences, however, remained fairly popular arguably  
268 until the mid-2000s. The focus of researchers in these fields was to find novel applications of ANNs across  
269 different earth and environmental problems.

270 It took until early 2010s before the third wave of popularity and interest in ANNs hit, when the field was  
271 revived and renamed ‘deep learning’. ‘Depth’ is a recently popularized term and loosely refers to the  
272 number of hidden layers in ANNs. A related term is ‘width’, which loosely refers to the number of neurons  
273 in hidden layers. Now, a DL model simply refers to an ANN with more than a few hidden layers. All of the  
274 recent excitement around ANNs is despite the fact that the structure, formulation, and other properties  
275 of MLPs have remained unchanged since their inception, except for some minor modifications. So, one  
276 might ask: is DL merely a repackaging and rebranding of what existed before? The next section attempts  
277 to answer this question while reviewing the recent milestones.

### 278 2.3. Latest developments and rebranding the field

279 To better understand the recent developments in the field of ANNs, one first needs to know the history  
280 around the ‘depth’ concept. MLPs, since their inception, have been used with various numbers of hidden  
281 layers, that is with various depths. Most applications, however, remained limited to networks with only  
282 one hidden layer until very recently. For example, Razavi et al. (2012a) report that more than 90% of ANNs  
283 used for surrogate modelling in water resources literature have only one hidden layer. There was (and  
284 perhaps still is) no consensus about a proper network depth, because identifying the optimal network  
285 configuration for a given problem and dataset is challenging.

286 Historically, some researchers favored ANNs with more than one hidden layer, arguing that they require  
287 fewer hidden neurons to approximate the same function (see e.g., Tamura and Tateishi, 1997). On the  
288 other hand, others asserted that single-hidden-layer ANNs are superior to those with more than one  
289 hidden layer with the same level of complexity (see e.g., de Villiers and Barnard, 1993). A discussion on  
290 this matter is available in Razavi et al. (2012a, pp 9-10).

291 Three general reasons historically drove interests towards ANNs with a single hidden layer: (1) the  
292 universal function approximation theorem (Hornik et al., 1989), as it provided a compelling argument that  
293 such ANNs are fully capable of learning any function; (2) the principle of parsimony, as ANNs with fewer  
294 hidden layers are generally deemed less complex and more understandable; and (3) difficulty of training,  
295 as ANNs with more hidden layers are more complex to train (see e.g., de Villiers and Barnard, 1993).

296 So, what recently shifted the status quo towards ANNs with multiple (typically many) hidden layers?  
297 Goodfellow et al. (2016) attribute the beginning of this shift to the work of Hinton et al. (2006), where  
298 ‘unsupervised learning’ was used to pre-train deep ANNs. They show unsupervised learning could  
299 effectively initialize the network’s parameters such that the subsequent training efforts through BP would  
300 become more successful. In AI, unsupervised learning refers to a process where a model learns from  
301 ‘unlabeled’ examples, which are technically inputs with no associated output. This is as opposed to  
302 ‘supervised learning’ where examples (i.e., data points) are ‘labeled’, meaning the output associated with  
303 each input is available; this process is called ‘model calibration’ in the context of process-based modelling.

304 Now, one might ask how unsupervised learning can be of any help in supervised learning. A common  
305 method for this purpose uses ‘autoencoders’, which are a class of ANNs historically used for  
306 dimensionality reduction and feature learning (Bourlard and Kamp, 1988). An autoencoder is an MLP,  
307 typically trained by BP, with one or more hidden layers that receives input and aims to produce the *same*  
308 input as its output. In a typical autoencoder, the middle layer has fewer neurons than the dimension of  
309 input, thereby acting as a bottleneck that encodes the input data in a lower dimensional space. The signals  
310 in the middle layer preserve the information contained in the inputs, which will be decoded back to the  
311 original space in the following layers. Autoencoders can pre-train some layers of a deep ANN such that  
312 the weights of those layers capture the main features in input data before passing them to the next layers.  
313 After the pre-training phase by unsupervised learning, the ANN needs to be further trained in the  
314 conventional supervised manner, using the actual output data and algorithms such as BP.

315 While the third wave of ANN popularity began by leveraging unsupervised learning to train deep ANNs,  
316 Goodfellow et al. (2016) argue the interest has gradually shifted back to the classic learning algorithms,  
317 such as BP, even for training deep ANNs. Those classic learning algorithms are now believed to work quite  
318 well in the DL context, perhaps due to the emergence of unprecedented computational power. In this  
319 regard, a game changer was the introduction of graphics processing units (GPUs) to the ANN community  
320 as a powerful tool to massively parallelize and thus expedite training algorithms (Raina et al., 2009). Such  
321 computational power has enabled the development of large ANNs, in terms of both depth and width. As  
322 such, ANNs with hundreds of millions (e.g., Devlin et al., 2018) or even a trillion parameters (e.g.,  
323 Rajbhandari et al., 2019) are becoming common.

324 Such a tremendous revival of the field of ANNs might seem at first surprising to those earth and  
325 environmental scientists who have known the field for a long time. This might be due, in part, to the fact  
326 that ANNs developed nowadays are fundamentally similar to those developed in the 1990s. Differences,  
327 if any in an application, are often in the details. For example, following Glorot et al. (2011), the tendency  
328 now is to use the rectified linear unit (ReLU), which is an unbounded function, instead of the standard  
329 ‘sigmoidal’ activation functions (see Eq. 1). The recent boom in data science and cyberinfrastructure and  
330 in investments by mega companies, such as Google, in this field might explain this revival, resulting in  
331 huge successes in image processing (Krizhevsky et al., 2017) and speech recognition (Young et al., 2018).  
332 Perhaps recent rebranding of the field under the title of ‘deep learning’ might have been in part a  
333 marketing strategy (Duerr et al., 2020); while as cited in Schmidhuber (2015a), this term was first  
334 introduced by Dechter (1986) to ML and by Aizenberg et al. (2000) to ANNs.

### 335 3. Geometrical Interpretation of DL

336 ANNs have always struggled with explainability and interpretability. Extensive research efforts have  
337 endeavored to peer inside the ‘black box’ of ANNs, via various forms of sensitivity analysis (see Section  
338 3.4 of Razavi et al. (2021) for a review) or geometrical or other types of interpretations (e.g., Benítez et  
339 al., 1997; Tickle et al., 1998; Castro et al., 2002; Wilby et al., 2003; Xiang et al., 2005; See et al., 2008; Razavi  
340 and Tolson, 2011; Samek & Müller, 2019). Despite all these advances, the issues around explainability and  
341 interpretability of ANNs, and of many ML techniques in general, are as relevant today as ever (see Rudin,  
342 2019).

343 This section utilizes a geometrical interpretation of ANNs to illustrate the internal functioning of ANNs  
344 and explain why deeper ANNs can be more powerful than ‘shallower’ ANNs in learning representations in

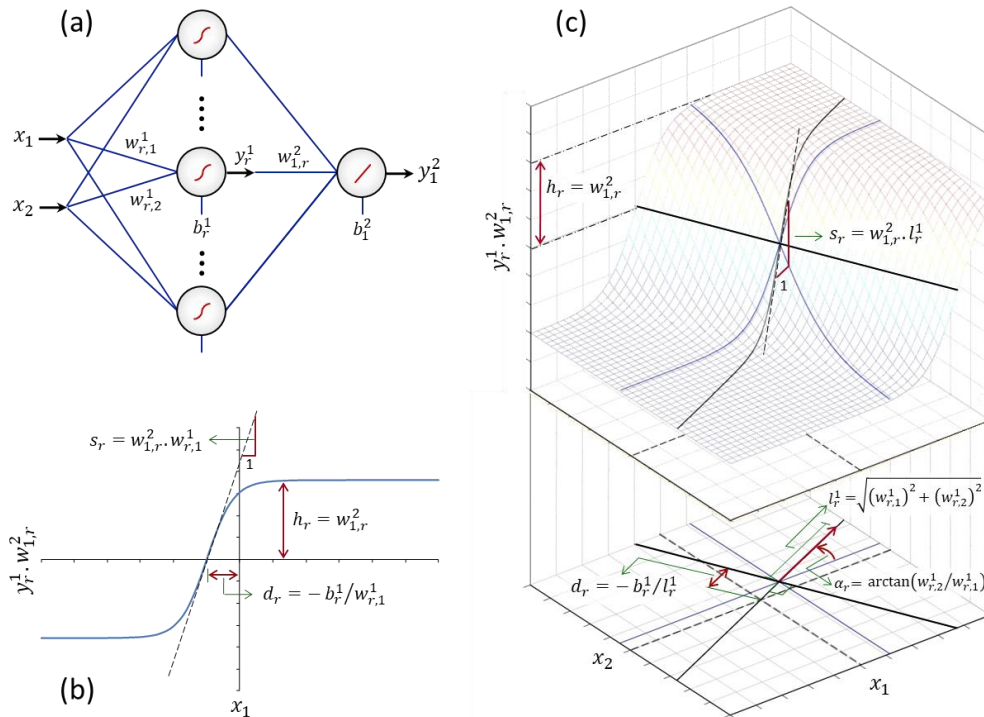
345 data. This interpretation is adopted in part from the work of [Razavi and Tolson \(2011\)](#), in which they recast  
346 ANNs with respect to a new set of more interpretable variables based on the network functional  
347 geometry.

### 348 **3.1. A perceptron**

349 An MLP is in principle made of a number of perceptrons. Consider an MLP with a single hidden layer with  
350 a sigmoidal activation function, as shown [Figure 2a](#). Each hidden neuron, e.g., the  $r^{\text{th}}$  neuron, is a  
351 perceptron whose output  $y_r^1$  is multiplied by the weight  $w_{1,r}^2$  before entering the output neuron. This  
352 hidden neuron, when only having one input  $x_1$ , forms a functional relationship such as that shown in  
353 [Figure 2b](#). This ‘sigmoidal unit’ can be characterized by three variables: ‘slope’, ‘location’, and ‘height’.  
354 There is one-to-one mapping between these variables and the original network variables,  $w_{r,1}^1$ ,  $b_r^1$ , and  
355  $w_{1,r}^2$ , as shown in the figure. As such, one can directly control the shape of the sigmoidal unit through  
356 slope, location, and height, and where needed, map them onto the network’s original variables. The  
357 benefit of doing so is that, unlike the original variables, the new variables are geometrically interpretable  
358 and therefore more intuitive.

359 [Figure 2c](#) shows the geometry of a perceptron with two inputs,  $x_1$  and  $x_2$ . In this case, the resulting  
360 sigmoidal unit forms a plane that can be characterized by slope, location, and height, plus an additional  
361 variable called ‘angle’ that specifies the direction toward which the sigmoidal unit is facing. This geometry  
362 can be extended to perceptrons with three or more (say  $D$ ) inputs, where the sigmoidal unit becomes a  
363 *hyperplane*, characterized by a slope, location, and height and  $D-1$  angles. Full details of this geometrical  
364 interpretation, and how it works in practice, are available in [Razavi and Tolson \(2011\)](#). Now let us see in  
365 the following how ANNs can approximate any function by putting together a large number of such  
366 sigmoidal units.

367



368

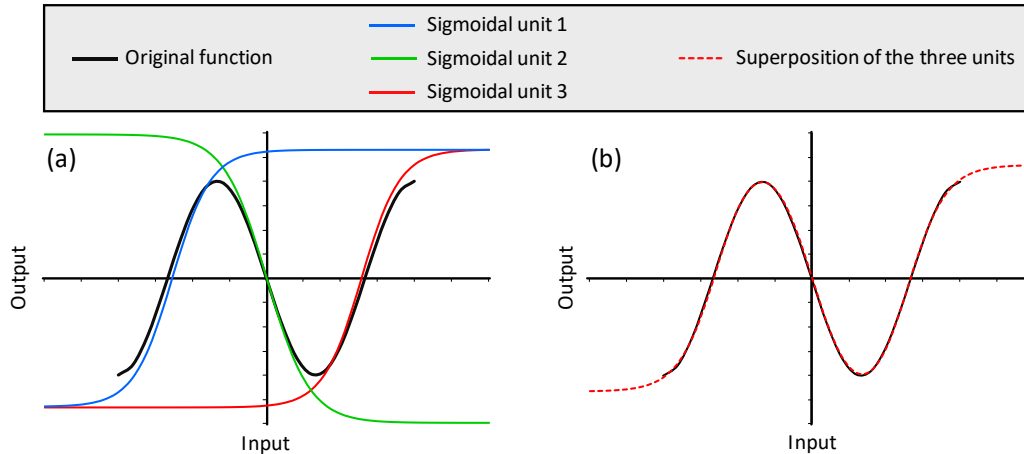
369 **Figure 2.** (a) An MLP with a sigmoidal hidden layer and linear output layer. (b) The sigmoidal line formed  
 370 by the  $r^{\text{th}}$  hidden neuron when the network has only one input,  $x_1$ . (c) The sigmoidal plane formed by the  
 371  $r^{\text{th}}$  hidden neuron when the network has two inputs,  $x_1$  and  $x_2$ . A sigmoidal line can be defined by three  
 372 variables that are related to the original weights and biases:  $h_r$  is the ‘height’ of the tails,  $s_r$  is the ‘slope’  
 373 of the tangent line at the inflection point, and  $d_r$  is the ‘location’ of the inflection point with respect to  
 374 the origin. A sigmoidal plane can be defined based on those three variables as well as  $\alpha_r$ , which is the  
 375 ‘angle’ of the normal vector perpendicular to the plane.  $l_r^1$  is the length of this vector. This geometry can  
 376 be extended to MLPs with any number of inputs (see Razavi and Tolson, 2011).

377

### 378 3.2. ANNs with one hidden layer

379 Single-hidden-layer ANNs are capable of approximating any function by combining, in parallel, as many  
 380 sigmoidal units as required. For example, suppose the underlying function to approximate is the sine  
 381 function shown in **Figure 3a**. Three sigmoidal units, with equal heights, equal absolute slopes, and  
 382 different locations, are required in parallel to represent the features of the function. These three units  
 383 can be produced by the hidden layer of an ANN and feed into a linear output layer, where they are  
 384 summed (superimposed) to approximate the sine function, as shown in **Figure 3b**.

385



386

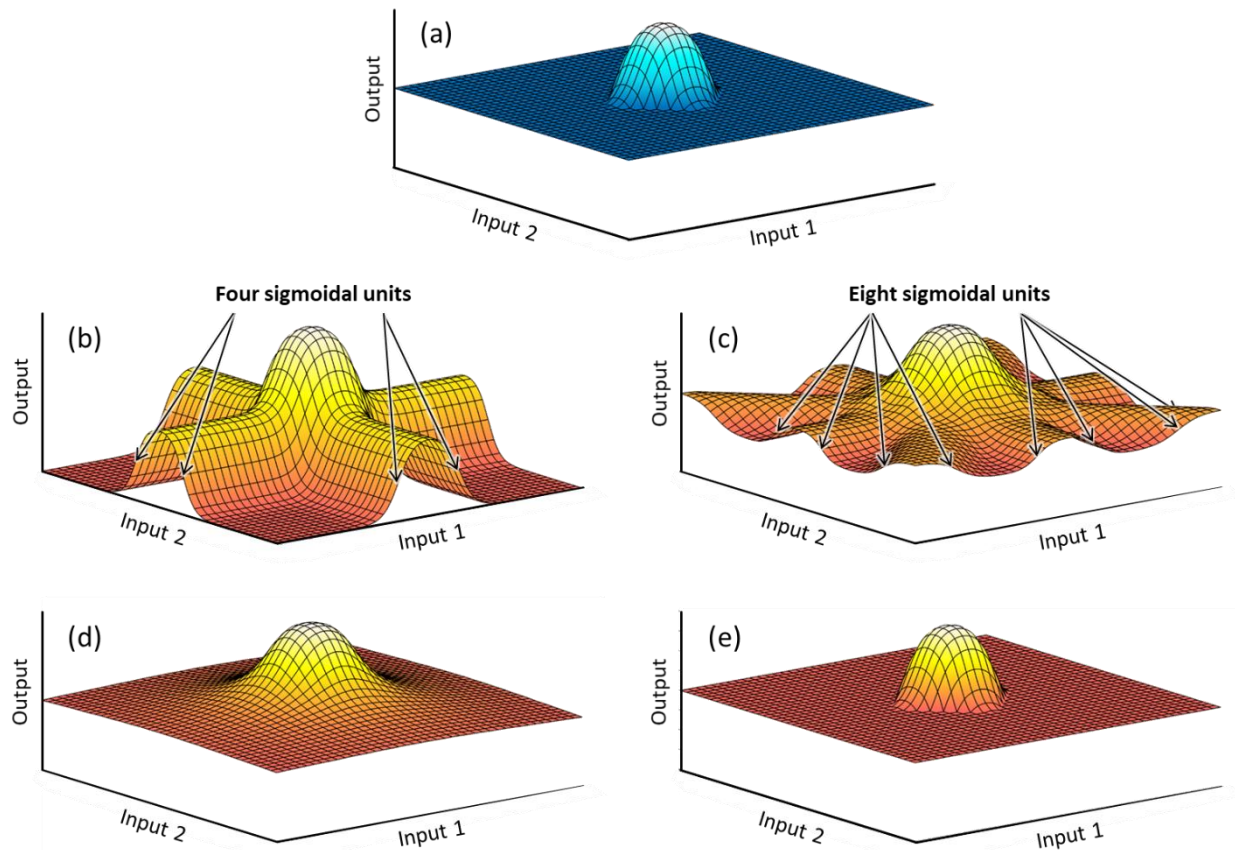
387 **Figure 3.** (a) An original sine function and three sigmoidal units, each approximating a part of the sine  
 388 function. (b) Output of the ANN that superposes the three sigmoidal units.

389

390 For problems with two or more inputs, the function approximation is not as straightforward. For example,  
 391 suppose the objective in a two-input problem is to approximate the dome-like feature shown in **Figure**  
 392 **4a**. A single-hidden layer ANN with four sigmoidal hidden neurons and one linear output neuron would  
 393 be able to approximate the dome part of the surface, as shown in **Figure 4b**. This ANN would basically  
 394 superimpose four sigmoidal units with equal heights, equal slopes, equal locations, but different angles  
 395 ( $90^\circ$  apart). The performance of this ANN, however, is unacceptable, as it creates erroneous features on  
 396 the tails.

397 But, can we rectify this issue by using more sigmoidal neurons? **Figure 4c** shows the performance of a  
 398 network with eight sigmoidal units, all having the same heights, slopes, and locations, but different angles,  
 399  $45^\circ$  apart. With more sigmoidal units at work, the performance at the tails is improved, producing less  
 400 erroneous features. Almost 40 hidden neurons are required, as shown in **Figure 4d**, to generate smooth  
 401 tails, similar to the original function shown in **Figure 4a**. This example provides a geometrical proof for the  
 402 universal function approximation theorem of **Hornik et al. (1989)** because, in principle, any function could  
 403 be approximated by a combination of such dome-like (i.e., basis) functions. The challenge, however, is  
 404 that many (possibly an excessively large number of) hidden neurons may be required for a given problem  
 405 to attain a desired level of approximation accuracy.

406



407

408 **Figure 4.** (a) Original dome-like function. Performance of ANNs with (b) four sigmoidal hidden neurons  
 409 and a linear output neuron, (c) eight sigmoidal hidden neurons and a linear output neuron, (d) 40  
 410 sigmoidal hidden neurons and a linear output neuron, and (e) four sigmoidal hidden neurons and a  
 411 sigmoidal output neuron.

412

### 413 3.3. So, why more than one hidden layer?

414 As proven by [Hornik et al. \(1989\)](#), and geometrically shown in the example above, ANNs with a sigmoidal  
 415 hidden layer and a linear output layer are capable of approximating any function with any desired level of  
 416 accuracy. So, one may wonder about the need to have deeper ANNs. This section attempts to answer this  
 417 question via an example.

418 Let us look back at the original function we aimed to approximate in [Figure 4a](#). Only four sigmoidal units  
 419 were required, as seen in [Figure 4b](#), to reproduce the dome-like feature at the center. One might ask: Can  
 420 we stick to these four sigmoidal units and somehow smooth the tails? Yes, all that is needed is a second  
 421 layer with a nonlinear activation function (e.g., sigmoidal) to deactivate any feature that is under a  
 422 threshold. In other words, in this process, the geometry formed by the sigmoidal units in the first layer  
 423 filters through another sigmoidal unit that bounds that geometry. [Figure 4e](#) shows how adding the second  
 424 non-linear layer enables the network to reproduce the original function, with only four neurons in the first  
 425 hidden layer. Similar to single-hidden-layer ANNs, those with two hidden layers can approximate any  
 426 function by putting the dome-like functions side by side.

427 In general, shallower ANNs are special cases of deeper ANNs. As shown in the example, deeper ANNs can  
428 provide more flexibility while they may require fewer hidden neurons across the network for  
429 representation learning. However, the training of deeper ANNs has been historically much more difficult  
430 because of the now well-known problem of ‘vanishing and exploding’ gradients. This problem relates to  
431 the fact that the partial derivatives of a loss function (Eq. 2) with respect to weights and biases in first  
432 layers, obtained via the chain rule of differentiation, tend to become very small (i.e., close to zero) or very  
433 large (i.e., exponentially growing or fluctuating). Improved algorithms along with higher computational  
434 power have now eased that difficulty and made possible the training of very deep ANNs (Schmidhuber,  
435 2015b).

436 Lastly, a related consideration about the proper number of hidden layers is about the fact that, in many  
437 problems, only a small part of the input space is active. In other words, some combinations of the different  
438 inputs might not occur in reality and therefore the accuracy of the ANN might not matter much in the  
439 regions of input space containing those combinations. For example, consider a case similar to one shown  
440 in Figure 4b, where the corners on the input space do not show up in the data available. A hydrological  
441 example is where snowfall and temperature are two inputs to ANNs. Because snowfall would never occur  
442 along with high temperature, the respective part of the input space always remains inactive.

#### 443 4. Relevance of Occam’s razor and equifinality?

##### 444 4.1. Issues with the complexity of ANNs

445 ANNs are known for their *hyper-flexibility* in fitting data, owing to their enormous degrees of freedom.  
446 For example, consider a problem with five inputs and one output. A single-hidden-layer ANN with 10  
447 hidden neurons would have 71 tunable parameters (60 weights and 11 biases), and adding a second 10-  
448 neuron hidden layer would result in a network with 181 parameters (160 weights and 21 biases). Compare  
449 that with linear or quadratic regression models for the same problem, which would have six or 21 tunable  
450 parameters, respectively. Such large degrees of freedom, manifest in large numbers of parameters,  
451 encountered in the field of ANNs do not seem consistent with a basic principle in statistical modelling:  
452 *Occam’s razor*.

453 Occam’s razor, or principle of parsimony, indicates that simpler hypotheses or models should be preferred  
454 over more complex ones. In other words, those models that serve the purpose with as few parameters as  
455 possible should be chosen. However, many data-driven modellers, in particular in the field of ML, have  
456 arguably abandoned Occam’s razor. For example, ANN users typically do not try simpler model types such  
457 as regression for the problem at hand. And, when using ANNs, they do not necessarily look for the most  
458 parsimonious network. Note that some literature proposes systematic approaches to choose a network  
459 structure based on growing, pruning, or other strategies (e.g., Reed, 1993; Teoh et al., 2006; Xu et al.,  
460 2006). In practice, however, such approaches have been of limited use and most ANN users choose the  
461 network structure on an *ad hoc* basis or by trial-and-error (see a survey by Razavi et al., 2012a). Recently,  
462 giant ANNs with hundreds of millions of parameters or more have become widespread (Devlin et al., 2018;  
463 Rajbhandari et al., 2019).

464 In addition, *equifinality*, a common and widely discussed issue in process-based modelling (Beven and  
465 Freer, 2001; Khatami et al., 2019), is not generally discussed or considered an issue in the context of ANNs.  
466 Equifinality concerns the fact that, in most cases, different model structures and parameter values can  
467 lead to similar modelling results. In other words, model structure and parameters are not uniquely

468 identifiable from data (Guillaume et al., 2019). This is despite the fact that, loosely speaking, the level of  
469 equifinality of ANNs is much larger than other types of models because of their massively parallel nature  
470 in producing model outputs.

471 So, how does DL handle the above issues? The answer is ‘indirectly’, by trying to avoid their undesired  
472 implications, which are *overfitting* and *lack of generalizability*. The former refers to a situation where a  
473 model fits the noise in the data rather than the underlying function. The latter refers to a case where the  
474 model does poorly in ‘out-of-sample prediction’, that is predicting situations unseen in the data used for  
475 model training. Various techniques are available in the ANN literature to address these issues, as outlined  
476 in the following.

#### 477 4.2. Leashing the hyper-flexibility of ANNs

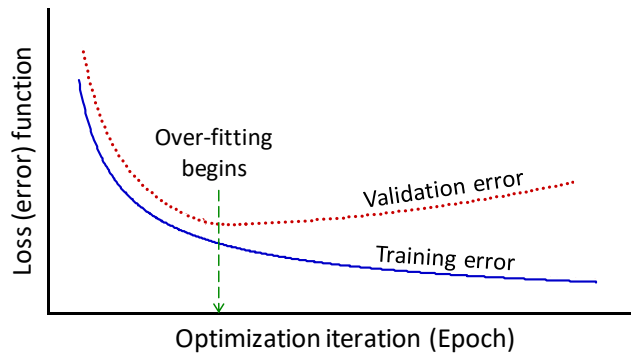
478 Techniques to control the hyper-flexibility of ANNs and to avoid overfitting fall under two general  
479 strategies, namely ‘early stopping’ and ‘regularization’. Before reviewing these strategies in this section,  
480 let us revisit the common data-splitting approach for calibration and validation of models.

481 ANNs and traditional, mechanistic models have major differences in terms of calibration and validation.  
482 In traditional modelling practices, the available data are commonly divided into ‘calibration’ and  
483 ‘validation’ datasets. The former is used to identify the model structure and parameters, while the latter  
484 is used to test the model performance in out-of-sample prediction.

485 In ANN practices, however, the available data are typically divided into three sets, commonly referred to  
486 as ‘training’, ‘validation’, and ‘testing’ datasets. Any data chosen for ‘training’ and ‘testing’ in the ANN  
487 context are respectively treated like ‘calibration’ and ‘validation’ datasets in the traditional modelling  
488 context. The third, ‘validation’ dataset in the ANN context is needed to leash the hyper-flexibility of the  
489 network while training. The simultaneous use of ‘training’ and ‘validation’ datasets during ANN training  
490 may be best described within the ‘early stopping’ strategy, as follows.

491 In the ‘early stopping’ strategy, the quality of fit to the ‘validation’ dataset is evaluated after each ‘epoch’,  
492 that is an optimization iteration trying to minimize the loss function on the ‘training data’ (see Section  
493 2.2). Empirically speaking, as the training error decreases over time, the validation error decreases as well  
494 for a while. However, at some particular epoch, the validation error may begin to increase while the  
495 training error may keep decreasing (see Figure 5). This epoch is deemed to mark the beginning of  
496 overfitting; thus, the user stops the training process. This strategy is therefore called ‘early stopping’ in  
497 the sense that the training stops early, before it can further improve the fit to the ‘training’ dataset (for a  
498 review, see Prechelt, 1998). When the training process stops, the generalizability of the trained network  
499 is assessed via out-of-sample prediction on the ‘testing’ dataset.

500



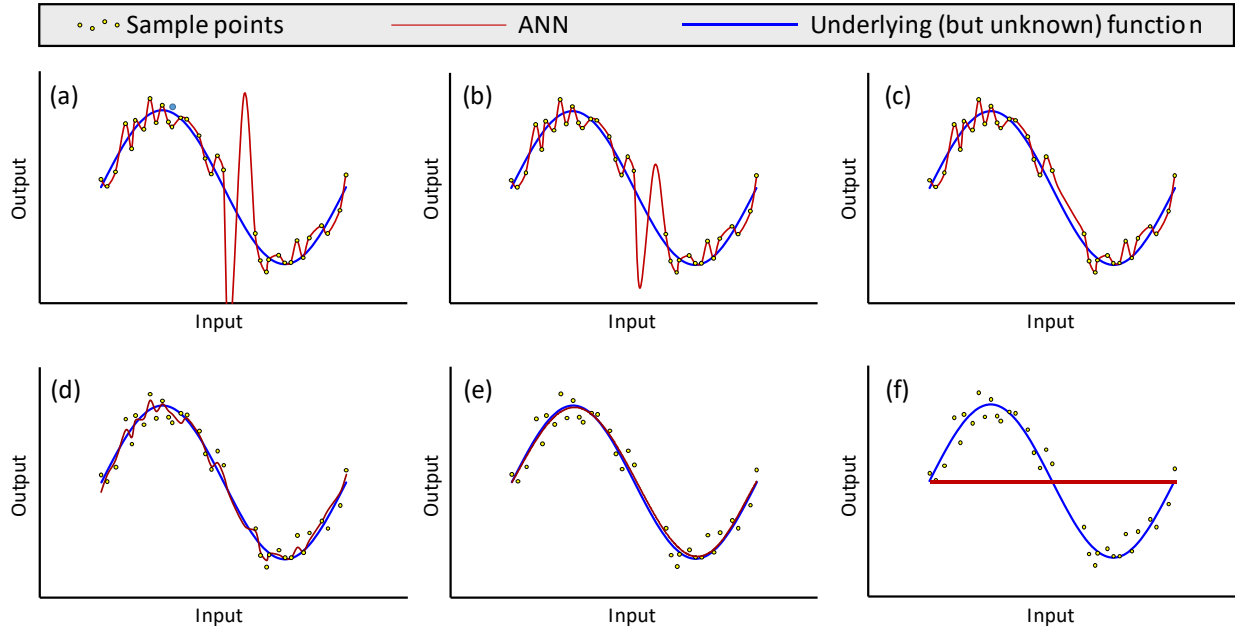
501

502 **Figure 5.** Illustration of ‘early stopping’. The loss function on the ‘training’ dataset generally decreases  
 503 with more epochs, whereas the loss function on the ‘validation’ dataset decreases early on but begins to  
 504 increase at some point, marking the commencement of overtraining.

505

506 ‘Regularization’ is another commonly used strategy to put a leash on the hyper-flexibility of ANNs. Unlike  
 507 ‘early stopping’, this strategy tries to minimize a ‘regularization function’ during training, to control the  
 508 ANN flexibility and tailor it to the problem at hand. This strategy has roots in the theory of ‘Tikhonov  
 509 regularization’ and typically views a more regularized model as one with a smoother response surface  
 510 (Tikhonov and Arsenin, 1977; Johansen, 1997). A traditional regularization function in the ANN context is  
 511 the sum of the square of all network parameters (Krogh and Hertz, 1991), based on the notion that, in  
 512 general, the smaller the parameters of a neuron, the less activated it is. For example, in an extreme case  
 513 where all parameters of a neuron are zero, that neuron becomes fully inactive and does not contribute a  
 514 feature to the overall network response. Razavi and Tolson (2011) provide a more efficient regularization  
 515 function, based on the geometry presented in Section 3, where the regularization function is the sum of  
 516 squares of all of the slopes. This regularization function only targets and removes the unnecessary  
 517 features, which are unsupported by data, from the overall network response.

518 But how can one balance the goodness of fit and smoothness of the network response? In practice, this  
 519 is a bi-objective optimization problem, where one objective is to minimize the error function and the other  
 520 is to minimize the regularization function. These two objective functions are commonly integrated into  
 521 one loss function via weighting schemes. Figure 6 shows how the two objectives compete in a real  
 522 example. Ideally, one may wish to achieve a performance such as that shown in Figure 6e. Doing so is not  
 523 trivial, however, because in practice the underlying function is unknown, available data are limited, and  
 524 response surfaces are multi-dimensional and cannot be easily visualized. The Bayesian regulation method  
 525 developed by MacKay (1992) and extended by Foresee and Hagan (1997) has proven useful to adaptively  
 526 assign the weights associated with each function during training.



527

528 **Figure 6.** Illustrative example of how regularization works to leash the hyper-flexibility of ANNs. Plot (a)  
 529 shows an extreme case with no regularization where the ANN overfits data. Plot (b) shows a case where  
 530 the regularization function is added to the loss function but marginally weighted. Plots (c) through (e)  
 531 show cases with incremental increases in the weight of the regularization function. Plot (f) shows the  
 532 other extreme case where the regularization function is dominantly weighted, making the ANN  
 533 effectively inactive. These plots are based on a real experiment, where the data sample was taken from  
 534 the underlying sine function shown and polluted with random noise.

535

536 A more advanced and recently developed regularization strategy is called ‘dropout’ (Hinton et al., 2012;  
 537 Srivastava et al., 2014). ‘Dropout’ is a heuristic, particularly designed for deep ANNs, that randomly  
 538 deactivates and then activates different neurons or groups of neurons at each epoch in the course of  
 539 training. When a part of an ANN is inactivated in this process, the resulting network is called a ‘thinned’  
 540 network. The ultimate prediction after training with dropout is viewed as an approximation of the  
 541 ensemble average of predictions by many independent ANNs. Basically, the many different thinned  
 542 networks created throughout the process are assumed to represent ANNs with different configurations  
 543 and parameters. This heuristic discourages neurons to co-adapt too much and, as such, is believed to  
 544 avoid overfitting.

545 **5. Fundamental differences from other ML methods**

546 **5.1. Local versus distributed representations**

547 Most ML methods, such as those based on kernel functions, are based on ‘local representations’. These  
 548 methods, while forming *connectionist* networks like ANNs, represent each entity (e.g., a training sample  
 549 point in the input space) via a single processing unit. For example, radial basis functions (Broomhead and  
 550 Lowe, 1988), Gaussian emulator machines (Kennedy and O’Hagan, 2000), and support vector machines  
 551 (Vapnik, 1998; Cherkassky and Ma, 2004) may use as many kernels as the number of training samples.

552 Each kernel typically has a limited radius of influence in the input space, and therefore only responds to  
553 inputs located in their local neighborhood.

554 Conversely, a unique feature of ANNs is their ability to learn through ‘distributed representations’ (Hinton  
555 et al., 1986). They typically represent an entity via collective efforts distributed among multiple processing  
556 units (e.g., sigmoidal units). Unlike kernel functions, the sigmoidal units typically have large regions of  
557 influence (see e.g., Figure 2c) that overlap each other in the input space (see e.g., Figure 4b). The former  
558 figure shows that a sigmoidal unit influences the entire input space, by dividing it into three zones: lower  
559 tail, upper tail, and slope. The latter figure shows how the influences of four such sigmoidal units are  
560 superimposed to generate the network response.

## 561 5.2. Implications for users

562 The use of distributed representations has several practical implications. To the author’s knowledge, these  
563 include:

- 564 • **Transparency:** The internal functioning of methods based on local representations is more  
565 transparent. Local representations are the most straightforward and easy-to-interpret way of  
566 learning, whereas distributed representations can be complex, often leading to emergent  
567 properties that cannot be easily explained by local representations (Hinton et al., 1986).
- 568 • **Learning difficulty:** Distributed representations are more difficult and time-consuming to learn.  
569 In local representations, the role of each processing unit may be assigned independently of the  
570 other units, but in distributed representations, many processing units may be configured together  
571 in complex ways to represent a feature in the data.
- 572 • **Network size:** Distributed representations need much smaller network sizes. In general, the size  
573 of the networks based on local representations is directly proportional to the size of the dataset,  
574 in most cases with a proportionality constant of one; that is, the number of processing units  
575 mirrors the number of training data samples. The size of networks based on distributed  
576 representations, however, depends on the complexity of features in the dataset, not its size.
- 577 • **Inexact interpolation or emulation:** Networks based on distributed representations are generally  
578 ‘inexact emulators’. This means they do not exactly fit the training samples to represent the  
579 features and patterns in the data. This is unlike some other ML methods, such as radial basis  
580 functions (Broomhead and Lowe, 1988) and Gaussian emulator machines (Kennedy and O’Hagan,  
581 2000), that are ‘exact emulators’, perfectly interpolating the training samples. Other inexact  
582 emulators include support vector machines (Vapnik, 1998; Cherkassky and Ma, 2004) and  
583 multivariate adaptive regression splines (MARS) (Friedman, 1991). Refer to Razavi et al. (2012a,  
584 Section 2.6.2) for a discussion on this issue.

585 In addition, ANNs are essentially multi-output models because they can have as many output neurons as  
586 required for a given problem. This means a single ANN can simultaneously predict different variables while  
587 accounting for their possible cross-correlations. Many other ML methods are, however, single-output  
588 models. For example, in the case of support vector machines, one need to develop two independent  
589 models to be able to predict two different variables in a system. Refer to Razavi et al. (2012a, Section  
590 2.6.5) for an extensive discussion on this matter.

## 591 6. How to introduce order, time-dependency, and memory

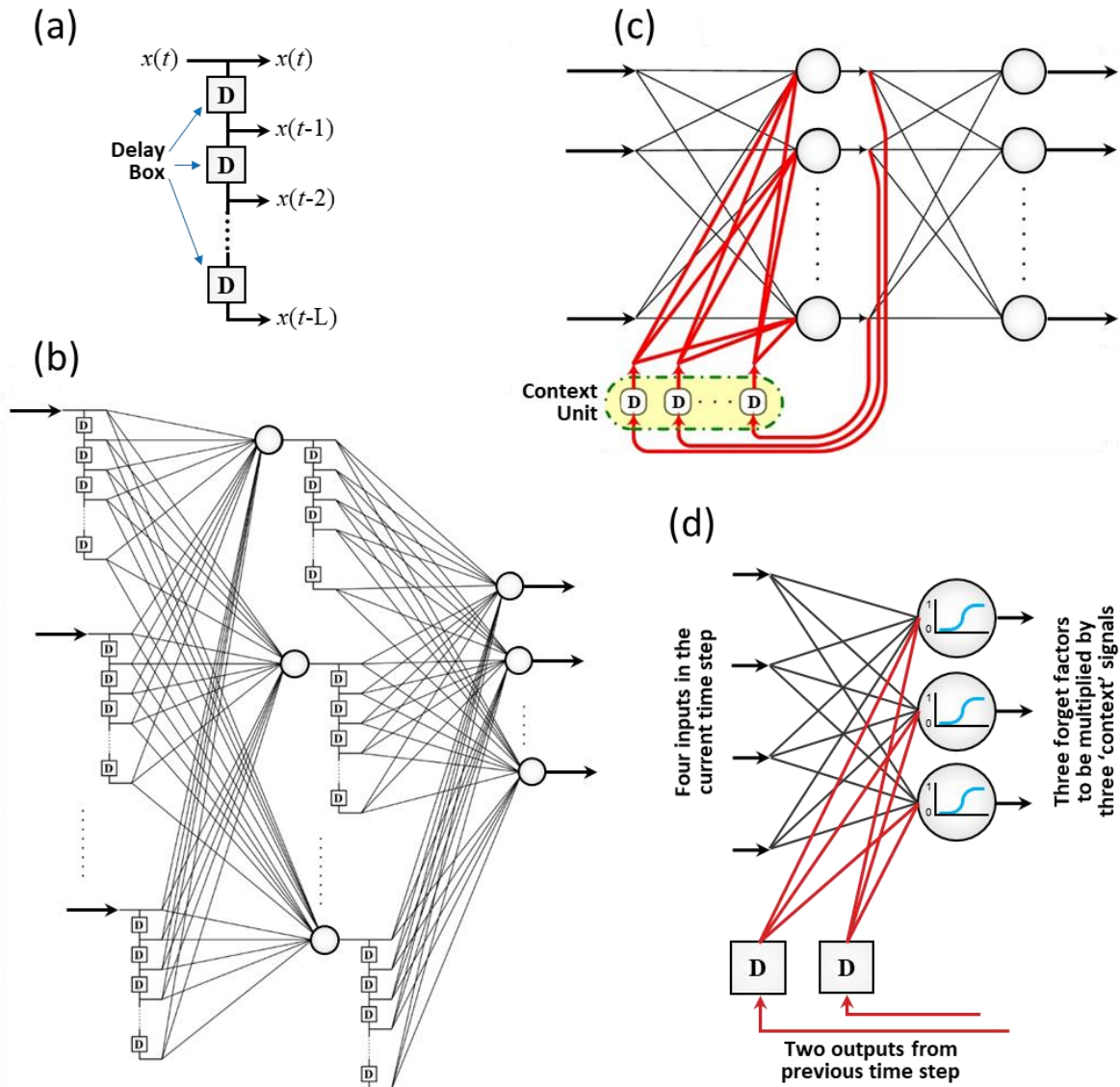
592 MLPs provide *static* mapping from inputs to outputs. However, many applications require mappings with  
593 a formal representation of time evolution and memory. To enable MLPs to do so, two general sets of  
594 tools, and combinations thereof, have been used in the literature: (1) tapped delay lines and (2) recurrent  
595 connections. These tools are explained in the following.

### 596 6.1. Tapped delay lines

597 A tapped delay line (TDL) consists of a certain number of time delay operators arranged in an incremental  
598 order (**Figure 7a**). TDLs can be installed on any internal connection weights of MLPs to represent time  
599 explicitly. The resulting ANN shown in **Figure 7b**, commonly referred to as a ‘time delay neural network’  
600 (TDNN; Waibel et al., 1989), has been widely used in a range of time-series processing applications. As  
601 such, TDNNs possess a *static memory with an adjustable length*. This length can be viewed as a  
602 hyperparameter to be tuned during training, along with network structural properties such as the  
603 numbers of layers and neurons in each layer.

604 Adding TDLs to an MLP significantly increases the number of tunable parameters. For example, a standard  
605 MLP with three inputs and 10 neurons in the first hidden layer would have 30 weights in that layer, while  
606 adding TDLs with a length of five to the inputs would result in an additional 50 weights (80 in total) to be  
607 trained.

608



609

610 **Figure 7.** (a) A tapped delay line (TDL), receiving the scalar  $x(t)$  at each time step  $t$  and outputting the  
 611 vector  $[x(t), \dots, x(t-L)]$ , where  $L$  is the length of the TDL. (b) A time delay neural network (TDNN) with one  
 612 hidden layer and TDLs installed on the input and hidden layers. (c) A recurrent neural network (RNN)  
 613 with one hidden layer and recurrent connections from the hidden neurons to themselves. In case of long  
 614 short-term memory (LSTM) networks, the context unit contains three 'gate layers' that adjust the  
 615 properties of the network's memory. (d) A gate layer of an LSTM with four inputs, two outputs, three  
 616 'context' signals that evolve through time steps.

## 617 6.2. Recurrent connections

618 TDLs, as described in **Section 6.1**, explicitly represent time with a memory unit of limited length. Unlike  
 619 TDLs, recurrent connections, first introduced by **Jordan (1986)**, enable ANNs to account for time evolution  
 620 based on an implicit memory concept, which is theoretically of unlimited length and is highly context  
 621 dependent (**Elman, 1990**). Recurrent connections receive the outputs of a layer at every time step and

622 feed them back to the same or some other layer in the next time step. Technically, they do so via a ‘context  
623 unit’ that stores those outputs in a set of delay boxes (**Figure 7c**). Recurrent connections can be installed  
624 on one or more layers (e.g., Jordan, 1986; Elman, 1990) or locally on some select neurons (e.g., Frasconi  
625 et al., 1992).

626 An MLP enabled with recurrent connections is commonly called a ‘recurrent neural network’ (RNN). An  
627 RNN can possess many more tunable parameters compared to an MLP with the same number of layers  
628 and neurons. Using the example given in **Section 6.1**, an MLP with three inputs and 10 neurons in the first  
629 hidden layer would have 30 weights in that layer, whereas adding recurrent connections to that layer  
630 (e.g., **Figure 7c**) would add 100 more weights (130 in total) to that layer.

631 Unlike TDNNs that possess a short-term memory, RNNs in theory can represent long-term dependencies  
632 in the input sequence as well. In practice, however, recurrent connections have difficulty representing  
633 long-term memory because they can easily get dominated by short-term memory. In other words, even  
634 very small features arising from short-term dependencies tend to mask features arising from long-term  
635 dependencies. In addition, RNNs are prone to the ‘exploding and vanishing’ gradients problem in their  
636 training (Bengio et al., 1994). This is because RNNs, even with a single hidden layer, are in principle deep  
637 networks implicitly possessing an infinite number of recursive layers.

### 638 **6.3. Gate layers to forget or preserve over time**

639 To explicitly account for and balance both short- and long-term dependencies in input sequences,  
640 Hochreiter and Schmidhuber (1997) introduced a new type of RNNs, called ‘long short-term memory’  
641 (LSTM). They extended and further parametrized the ‘context’ (also called ‘cell’) such that the network  
642 can more explicitly control what information to hold over time and what to forget. The LSTM’s context  
643 unit modulates not only the outputs in the previous time step but also the inputs to the network in the  
644 current time step. It does so via three independent layers of neurons arranged in the so-called ‘forget  
645 gate’, ‘input gate’, and ‘output gate’ layers. The neurons of each ‘gate layer’ as shown in **Figure 7d**, at  
646 each time step, receive recurrent connections as well as the new input to the network, and generate their  
647 response between *zero* and *one* via using a logistic function. These responses are then multiplied by their  
648 respective signals flowing through the context, which means a value of zero would kill a signal whereas a  
649 value of one would fully preserve it. Due to the additional weights and biases in the gate layers, an LSTM  
650 typically has many more tunable parameters than a conventional RNN.

651 LSTMs are now perhaps the most popular and widely used type of ANNs with memory. However, LSTMs  
652 took a long time (more than a decade) to become known and mainstream, particularly beyond their core  
653 computer science community. Their widespread application nowadays owes to recently developed  
654 software tools such as Python’s *TensorFlow* that efficiently implement variations of LSTMs for a range of  
655 problems.

### 656 **6.4. Training considerations when the order of data matters**

657 The training of memory-enabled ANNs, such as TDNNs, RNNs, and LSTMs is different from that of standard  
658 ANNs in terms of the way time-ordered data are presented to the network. To train standard ANNs, the  
659 data entries can be presented in any order even randomly, for example through stochastic gradient  
660 descent (Bottou, 2010). In memory-enabled ANNs, however, the data entries should be presented in order

661 of occurrence so that the structure of the time dependency is preserved. While this point might seem  
662 trivial, it requires careful attention in practical applications.

663 Another point to consider in the training of memory-enabled ANNs is that all data entries are typically  
664 viewed to have equal importance, regardless of their location in the sequence. When used in an online  
665 operational forecast, however, the ‘forgetting factor’ approach can be used to discount older samples.  
666 This approach allows the network to adapt to non-stationary environments, where more recent data are  
667 more representative of the underlying processes than older data (Razavi and Araghinejad, 2009).

668 Lastly, elements of TDNNs and RNNs can be combined in a variety of ways. A well-known combination is  
669 ‘time-delay recurrent neural networks’ developed by Kim (1998) and used in various applications such as  
670 long-term precipitation forecasting in Karamouz et al. (2008); see Razavi and Karamouz (2007) for a  
671 comparison of MLP, TDNN, RNN, and TDRNN in the context of flood forecasting. While such combinations  
672 may show improved modelling power compared to other ML or statistical methods, the attribution of  
673 memory gains to the different elements can arguably be challenging, if possible at all.

## 674 7. ML versus process-based modelling – An experiment

675 ML has been extensively used to model systems for which process-based models are also available.  
676 Process-based models are based on the physics governing the underlying processes and are therefore  
677 typically evaluated based on both their physical realism and goodness of fit to data. ML, however, does  
678 not do much, if anything, with the underlying physics while reportedly doing a superior job in fitting data,  
679 even in out-of-sample prediction. A fairly large body of literature benchmarks ML techniques, particularly  
680 ANNs, against process-based models. Examples of such comparisons (directly or indirectly) in the context  
681 of hydrologic modelling include Hsu et al. (1995), Tokar and Markus (2000), Wilby et. (2003), Kratzert et  
682 al. (2018), Kratzert et al. (2019), Feng et al. (2020), and Ma et al. (2021). Some studies, such as Wilby et  
683 al. (2003), also detected correlations between the weights of an ANN and state variables of a process-  
684 based hydrologic model as a way to verify that their ANN can capture the underlying processes in a  
685 hydrologic system.

686 This section provides an experiment that runs and compares both types of models for the same problem  
687 and walks the reader through all of the steps involved. In particular, the processes around calibration and  
688 validation, role of physics, and interpretations of out-of-sample prediction are discussed. This experiment  
689 is performed in the context of hydrologic modelling, which has seen tremendous progress over the years  
690 with respect to both ML and process-based modelling.

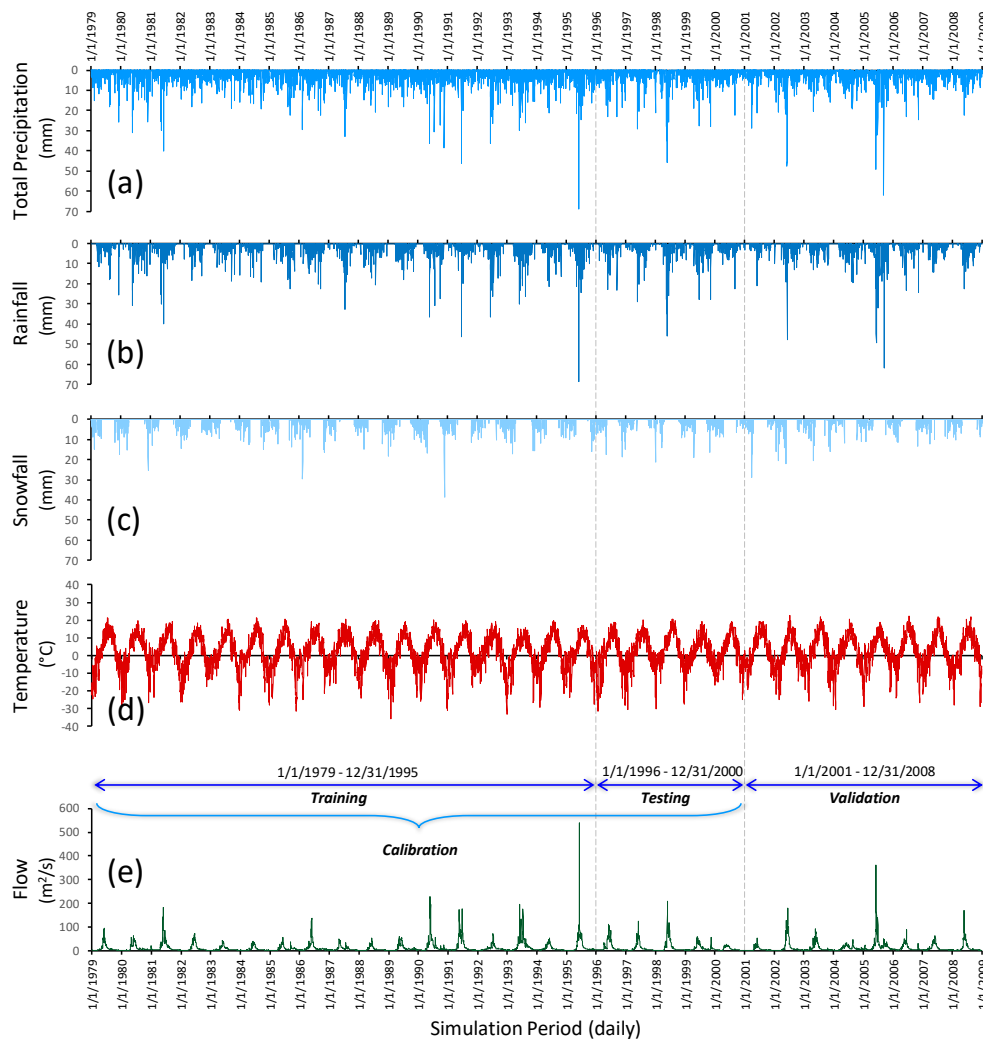
### 691 7.1. Data and models

692 The case study used aims to model the hydrologic system of the Oldman River watershed in Alberta,  
693 Canada. This watershed has an area of 1434.73 km<sup>2</sup> at Waldron's Corner with a long-term average  
694 temperature of 2.2 °C. On average, this watershed receives 611 mm of precipitation (rainfall + snowfall)  
695 annually and generates 11.7 m<sup>3</sup>/s of river flow. Figure 8 shows the 30-year long daily time series data  
696 used. The first 22 years were used for model ‘calibration’ (i.e., the ‘seen’ data in model development) and  
697 the last eight years for model ‘validation’ (i.e., the ‘unseen’ data in model development). The first three  
698 months of the calibration period were used for model spin-up. In the case of DL, the calibration period  
699 was further broken into ‘training’ (17 years) and ‘testing’ (5 years) periods, the latter for early stopping of

700 the training process to avoid overfitting. Note that, as explained in **Section 4.2**, the naming convention in  
701 the DL context for the ‘validation’ and ‘testing’ periods is often the other way around.

702 To model this system, an LSTM configuration was chosen here as a state-of-the art DL model that accounts  
703 for time dependency and memory. The inputs to the LSTM model are daily precipitation and temperature  
704 (**Figures 8a and d**) and the output is the concurrent flow (**Figure 8e**). The LSTM structure was rather  
705 arbitrarily chosen to have one hidden layer with five neurons, resulting in 166 calibration parameters. For  
706 benchmarking purposes, a classic hydrologic model called HBV (**Lindström et al., 1997**), as implemented  
707 in HBV-SASK (**Razavi et al., 2019**), was used. HBV-SASK is based on a conceptualization of physical  
708 principles governing the water movement in a watershed using 12 calibration parameters. Each of these  
709 parameters has a physical interpretation and a physically justified feasible range (see **Figure 9 and Table**  
710 **2 of Razavi et al., 2019**). Full detail (including data) of this Oldman River watershed case study, which has  
711 been developed for educational purposes, is available in **Razavi et al. (2019)**.

712



713

714 **Figure 8.** Dataset used for the modelling experiment with ML and mechanistic modelling. (a) Measured  
715 precipitation time series (rainfall + snowfall). (b) Estimated rainfall time series (precipitation when

716 temperature  $\geq 0$  °C). (c) Estimated snowfall time series (precipitation when temperature  $< 0$  °C). (d)  
 717 Measured temperature time series. (e) Measured river flow time series. The training period was used for  
 718 LSTM training, while the testing period was used for early stopping. The calibration (training + testing)  
 719 period was used for HBV calibration. The validation period was used to evaluate the performance of  
 720 both LSTM and HBV in out-of-sample prediction.

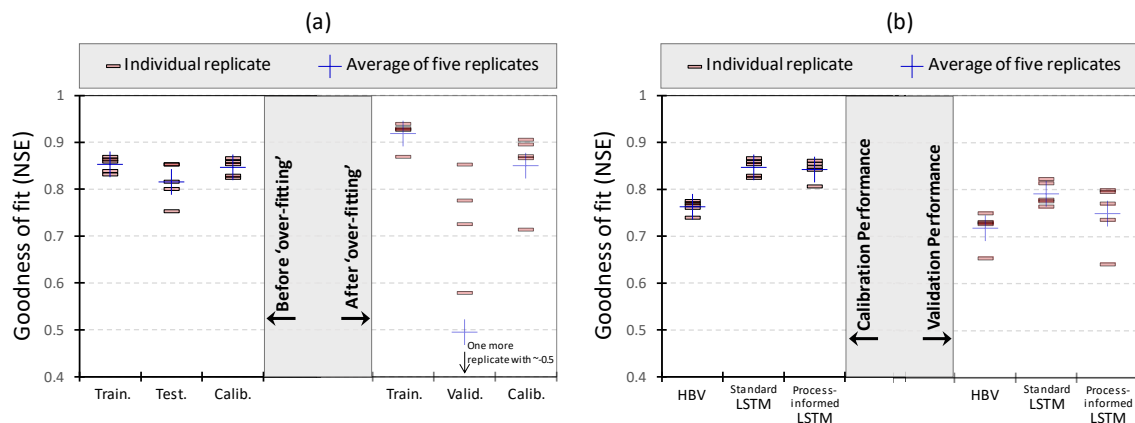
721

722 **7.2. Model performance in calibration**

723 The model calibration problem was cast as an optimization problem that tries to maximize the goodness  
 724 of fit to data by tuning the model parameters, with the Nash-Sutcliffe efficiency (NSE; Nash and Sutcliffe,  
 725 1970) as the objective function. NSE is essentially a normalized version of mean squared errors computed  
 726 as  $1 - [\text{VAR}(\text{errors})/\text{VAR}(\text{observations})]$ . As such, an NSE of one indicates a perfect fit, and an NSE of zero  
 727 indicates the model prediction is not any better than the average of observations. As a rule of thumb,  
 728 hydrologists often call an NSE of 0.7 and higher an acceptable fit.

729 The LSTM model was calibrated using BP with the early-stopping strategy to avoid overfitting. In each  
 730 epoch, the training period data were used to update the network parameters, while the testing period  
 731 data were used to detect possible overfitting. Five independent replicates of LSTM calibration (with  
 732 different initial random seeds) were conducted to account for possible variability of model performance.  
 733 **Figure 9a** shows the training results of the five replicates compared to a case where the training would  
 734 not have stopped. As expected, the LSTM performance keeps improving in training, whereas in testing it  
 735 begins to significantly degrade at some point. The objective function in training came very close to one  
 736 after many more epochs but with very poor performance in testing (not shown).

737 The HBV-SASK model was calibrated by a multi-start Newton-type optimization algorithm. Similar to  
 738 LSTM, five independent replicates of HBV-SASK calibration were run. **Figure 9b** compares the performance  
 739 of HBV-SASK with that of LSTM in calibration. At this point, only check the performance of the ‘standard’  
 740 LSTM model in calibration. The figure shows all five replicates of LSTM outperform those of HBV-SASK.  
 741 Note that the calibration performance of HBV-SASK shown herein is almost the best the author has  
 742 achieved so far for this watershed. Based on these results, the superiority of LSTM over HBV-SASK in  
 743 calibration is quite significant from a hydrologic modeling point of view. The performance of the two  
 744 models in validation is discussed in **Section 7.4**, but before that let us discuss what information the two  
 745 contained prior to calibration.



746

747 **Figure 9.** (a) The performance of LSTM in training, testing, and calibration (training + testing) periods  
748 before and after ‘overfitting’. Training of each replicate was stopped once overtraining began at epoch  
749 numbers ranging from 30 to 110 (left panel). Then, each replicate continued to complete 250 epochs in  
750 total to merely evaluate the impact of overfitting (right panel). (b) A comparison of LSTM and HBV in  
751 out-of-sample prediction. Standard LSTM and process-informed LSTM are discussed in **Sections 7.4 and**  
752 **7.5**, respectively.

### 753 **7.3. What about *a priori* information encoded in models?**

754 At this point, let us step back and investigate what we have achieved in terms of learning from data for  
755 both the LSTM and HBV-SASK models. The development of the LSTM model was not based on any *a priori*  
756 knowledge of how a watershed system works and the governing physical principles. As such, the model  
757 learned everything from scratch merely using examples from data. Basically, the model started with a fully  
758 randomized internal configuration controlled by a large number (i.e., 186) of parameters and then tuned  
759 those parameters to adapt the internal functioning of LSTM to the underlying real-world system  
760 represented in the data. **Figure 10a** shows the LSTM performance of arbitrarily chosen replicates before  
761 and after calibration. The model response to inputs before calibration seems to be completely random  
762 but, after calibration, the model response has learned to closely follow the underlying system response.

763 Unlike LSTM, HBV-SASK encodes the expert knowledge available in the field of hydrology. This model is a  
764 collection of conservation of mass equations and process parametrizations that represent how  
765 hydrologists conceptualize the way a watershed works. This ‘physically based’ modelling structure is  
766 presumably able to emulate the behavior of any watershed by tuning only 12 parameters. **Figure 10b**  
767 shows how the model performs before calibration, with parameter values chosen to be at the midpoint  
768 of their ranges, and after calibration. The figure shows the ‘uncalibrated’ model responds reasonably to  
769 the inputs; it generally captures the timing of flows and emulates the low flow segments well but is overly  
770 responsive to large precipitation events, generating spurious spikes in flows. Calibration, either manual  
771 by expert knowledge or automatic as done here via optimization, can fix the discrepancies and fit the  
772 model output to observations.

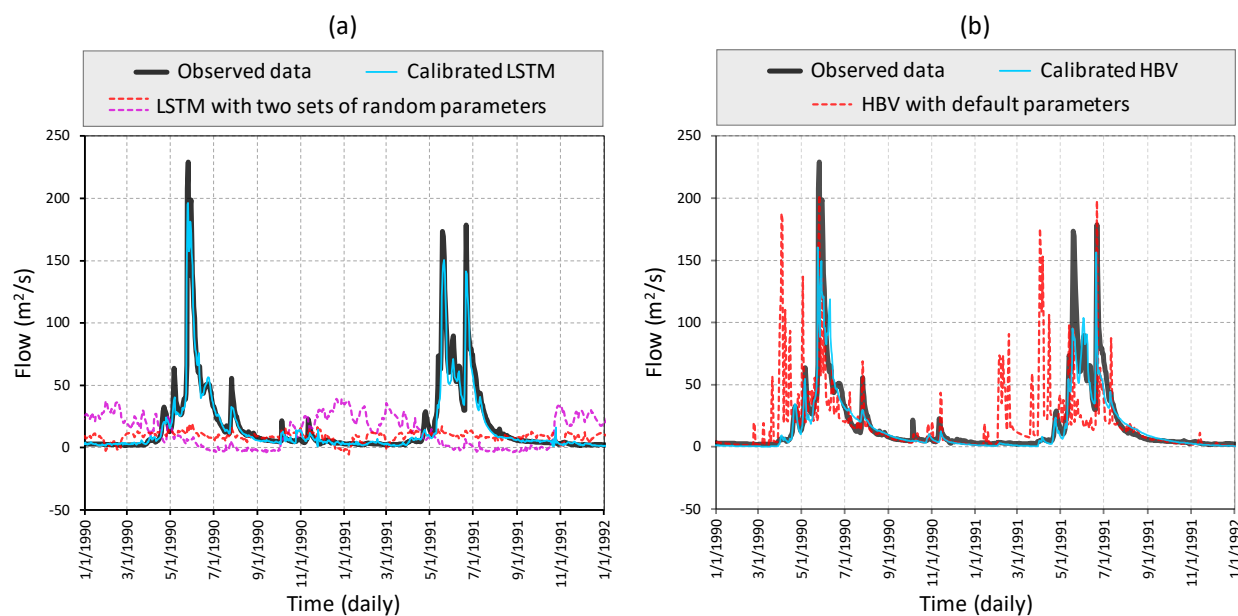
773 So, a fundamental difference between the two approaches is now clearer: using a process-based model  
774 is about directly using a wealth of expert knowledge available in a scientific field while using DL is about  
775 learning everything from scratch directly from data. This difference is manifest in the number of  
776 parameters that need to be tuned to achieve a reasonable performance. Notably, the LSTM model  
777 achieved a better performance in emulating observations after calibration, as evident in a comparison of  
778 **Figures 10a and b**. However, in any modelling exercise, one needs to ensure the model gives the right  
779 answer for the right reasons (**Kirchner, 2006**). That is why proper model evaluation in out-of-sample  
780 prediction is critically important, as discussed in the next section.

### 781 **7.4. Model validation: Standard versus true out-of-sample prediction**

782 In general, validation and verification of mathematical models are very challenging in some scientific  
783 disciplines, if possible at all (**Oreskes et al., 1994**). The standard practice, however, is to test the  
784 performance of the model under investigation in terms of reproducing some historical record not seen  
785 during model calibration (**Klemeš, 1986a**), a process called ‘out-of-sample prediction’ in this paper. **Figure**  
786 **9b** shows the results of such practice in the validation period set in **Figure 8**. In this case, both LSTM  
787 (standard) and HBV models do reasonably well from a hydrologic point of view, with LSTM outperforming

788 HBV across all replicates. In addition, and as expected, both models produced slightly lower NSE values in  
789 validation compared to those in calibration.

790 The above so-called ‘model validation’ is inherently partial (Oreskes et al., 1994). While the performance  
791 of LSTM appears to be better than that of HBV in a ‘relative’ sense, one needs to take extra care before  
792 making such a conclusion. As argued by Klemeš (1986a) more than three decades ago, a strong  
793 assumption in this type of validation is that the conditions under which the model will be used will be  
794 similar to the conditions under which the model has been developed and calibrated. It is now well-  
795 recognized that such an assumption may not hold, as many natural systems are essentially non-stationary  
796 (Milly et al., 2008; Razavi et al., 2015). Despite such recognition, this standard model validation practice  
797 has arguably remained unchanged (Beven, 2018).



798  
799 **Figure 10.** What does a model learn via calibration? Performance samples of (a) LSTM and (b) HBV  
800 before and after calibration for a select two-year period.

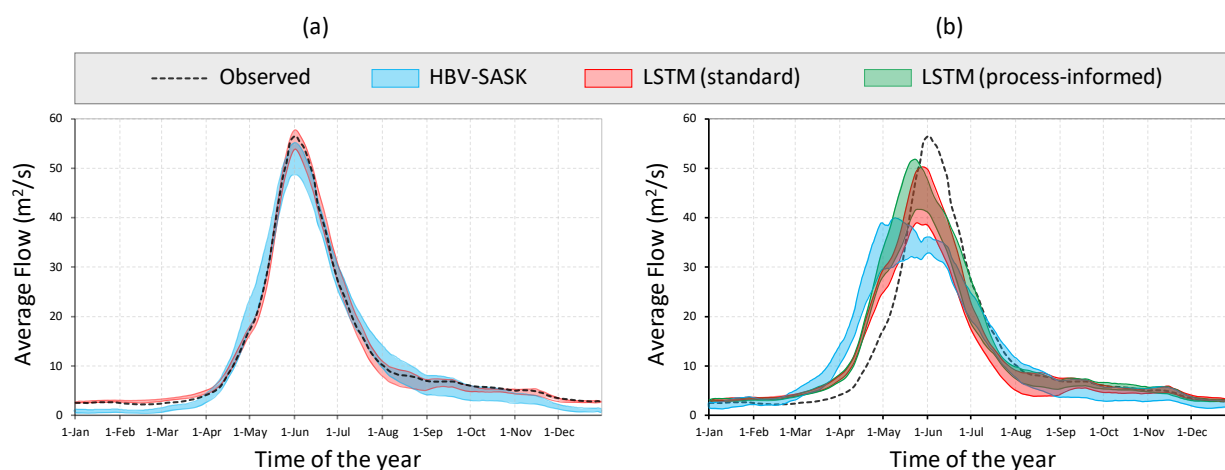
801  
802 Here, I took a sensitivity analysis approach via a *what-if scenario* question to test and compare the  
803 performance of both models in a ‘true’ out-of-sample prediction, basically under conditions that have not  
804 truly been seen in the process of model development and calibration. The question is how the system  
805 would behave if the average temperature warmed by 2 °C while everything else remained the same. To  
806 assess this scenario, both calibrated models were fed a new temperature time series obtained by adding  
807 2 °C to all daily temperature values of Figure 8d. These new ‘synthetic’ inputs roughly provide a picture of  
808 what might happen in this watershed under global warming. The modelling results under such scenarios  
809 are typically used to inform policy making for climate change adaptation.

810 Now let us use the two different models to evaluate the possible changes in the watershed behavior in  
811 response to a 2 °C warming. Here, instead of looking at individual simulated time series, the possible  
812 change in the average seasonality of flows is of interest. First, look at Figure 11a to check the consistency  
813 of simulated flows for the historical period. Both models generally follow the observed seasonality, but

814 the range provided by the LSTM model is generally narrower and better encapsulates observations in both  
815 low and high flows.

816 Under the new conditions, however, the two models show the two distinct behaviors shown in **Figure**  
817 **11b**. According to LSTM, peak summer flows would decline by about 25% on average and the time of the  
818 peak would shift backward by about a week, from the beginning of June to a time in the fourth week of  
819 May. According to HBV-SASK, however, the changes would be more pronounced. The peak flows would  
820 decline by about 35% on average and the flows might show two modes: the higher one at the beginning  
821 of May and the other at the beginning of June, at about the same time as the peak in the historical  
822 observations. Are such differences not sufficiently large so as to make the user skeptical about the  
823 modelling process?

824



825

826 **Figure 11.** Long-term average daily flows throughout the year under (a) historical and (b) hypothetical  
827 conditions. The envelopes represent the daily ranges of flows obtained by the five replicates of each  
828 model. The curves were smoothed by a 20-year moving average filter.

829

### 830 7.5. Injecting some physics into ML

831 At this point, one may wonder about the possibility of ensuring that DL results be physically consistent,  
832 particularly under new conditions. Let us give it a try by recasting the modelling problem based on some  
833 understanding of the governing physics in hydrology. For example, physics tells us that the freezing point  
834 of water is around 0 °C and, therefore, this threshold could be used as an approximation to differentiate  
835 rainfall from snowfall on a daily basis, i.e., if the temperature on a day is above/below 0 °C, the  
836 precipitation on that day, if any, is considered to be rainfall/snowfall (see **Figures 8b and c**). This  
837 differentiation is actually a part of process parameterization in HBV, similar to many other hydrologic  
838 models, via a parameter called ‘temperature threshold’ (TT) for melting/freezing and separating rain and  
839 snow, with a feasible range from -4 to +4 °C (see **Razavi et al., 2019** for details). The warming of a  
840 watershed would naturally change the rainfall to snowfall ratio, and so integrating this domain knowledge  
841 with the LSTM model makes sense.

842 Perhaps the most straightforward way of introducing the TT concept to LSTM is via pre-processing of the  
843 inputs. Therefore, a new LSTM model was developed and calibrated, called ‘process-informed LSTM’ in  
844 this paper, with three inputs: rainfall, snowfall, and temperature as shown in **Figures 8b, c, and d**. Similar  
845 to the original, the new LSTM model has one hidden layer with five neurons, resulting in 186 calibration  
846 parameters. The procedure for the calibration and validation of the process-informed LSTM was the same  
847 as for the ‘standard LSTM’, already explained in **Sections 7.2 and 7.4**. **Figure 9b** compares the performance  
848 of the process-informed LSTM with HBV and the standard LSTM. The figure shows the two LSTM models  
849 perform comparably well. Process-informed LSTM results in a slightly lower average NSE in validation but,  
850 with only five replicates, this small difference should be interpreted with caution.

851 **Figure 11b** demonstrates the performance of the process-informed LSTM model in the ‘true’ out-of-  
852 sample prediction. According to this model, the summer peak flows would decline by 20% on average and  
853 the time of peak would appear about two weeks earlier than in the historical record, in the third week of  
854 May. The process-informed LSTM model generated rising and falling limbs that are more consistent with  
855 those of HBV-SASK. Overall, however, the results of HBV-SASK under the new conditions are still quite  
856 different.

#### 857 **7.6. So, what model should we trust: the ML or process-based model?**

858 Now the question is which one of the three models produced the most credible picture of possible  
859 watershed behavior under the new conditions. In practice, this question is very difficult to answer, if  
860 possible at all. In general, the prediction of such changes can be debated and might vary from one study  
861 to another, depending on the models and data used and disciplinary views. Perhaps, a definite answer  
862 would need to wait until the future has come and shown such possible changes. And, from a bigger-picture  
863 point of view, models of natural systems cannot be verified or validated in true out-of-sample prediction,  
864 because those systems are never closed and not everything can be represented in a model, as argued by  
865 **Oreskes et al. (1994)** nearly three decades ago.

866 But, as scientists, we have our own perceptions and intuitions. These might be biased but still useful to  
867 provide a ground for building confidence in the credibility of a model. In the context of the case study  
868 given, previous research on the Canadian Rocky Mountains has indicated that warming *alone* will result  
869 in a considerable reduction in flows and earlier peaks in watersheds similar to the Oldman River  
870 watershed. A synthesis of research efforts under the Changing Cold Regions Network (CCRN; **DeBeer et**  
871 **al., 2021**) on the cold interior of western Canada indicates a shift in timing of the spring hydrograph rise  
872 and peak flows of nearly two weeks earlier by mid-21<sup>st</sup> century, and as much as one month by the late  
873 21<sup>st</sup>-century. These projections, which themselves are based on rigorous atmosphere-landsurface  
874 modelling, are consistent with the modelling results presented in the previous sections but cannot  
875 pinpoint the most accurate model.

876 What is worrisome is the large divergence in behavior of models in response to expected, but yet to be  
877 seen perturbations, whereas those models produce comparable results in standard out-of-sample  
878 prediction. Broadly speaking, one might say any known consistency of a model with the known underlying  
879 physics can improve model’s explainability and interpretability, thereby helping us better explain the  
880 model behavior in response to such perturbations. Explainability and interpretability are fundamental  
881 assets in building trust in a model, and of course, physically-based models are advantaged in that respect.  
882 I would say mistrust in some data-driven modelling paradigms such as ANNs is a long-standing issue in  
883 part of our research community and stakeholders. I have heavily struggled with this issue as a researcher

884 who started his research career with ANNs almost 20 years ago and has also had the privilege to work  
885 extensively with process-hydrologists and physically-based modellers. I believe with the current  
886 momentum and excitement, an opportunity is arising to bring the two world views together and promote  
887 the dialogue between the champions of process-based modelling and those of machine learning, as  
888 already discussed by many authors (e.g., Reichstein et al., 2019). Doing so, however, requires an in-depth  
889 understanding and appreciation of the value of domain knowledge, as discussed in the next section.

## 890 8. Discussion

### 891 8.1. What is the typically ignored value of domain knowledge in DL?

892 True out-of-sample prediction is nothing but ‘extrapolation’ beyond the observed data and behaviors used  
893 in model development and calibration. Extrapolation is a reality that many predictive models nowadays  
894 must face because of ‘non-stationarity’ in climate and the environment (Milly et al., 2008; Razavi et al.,  
895 2015). Any purely regression-type model, including those arising from DL, would be disadvantaged in  
896 extrapolation as, by definition, extrapolating would require working in parts of the problem space for  
897 which they have not received any information. Conversely, mechanistic models may be salvaged in  
898 extrapolation by the domain knowledge encoded within them.

899 But what does domain knowledge offer when it comes to extrapolation? The answer is the set of principles  
900 modulated via conservation laws (e.g., mass, energy, and momentum) and process parametrizations,  
901 which represent our perceptions of how two or more variables might be related (Gupta et al., 2012). Such  
902 principles have been developed and evolved over time based on extensive observation and research by  
903 scientists and practitioners. The *limits of validity* of such principles are typically known. In the following,  
904 the importance of taking advantage of those principles in modelling and prediction is discussed with  
905 respect to three aspects: conservation laws, monotonicity and rates, and feedback mechanisms.

906 **Conservation laws:** In physics, a conservation law states that a specific measurable property does not  
907 change within an isolated system with time. Such a law is usually expressed as a ‘continuity equation’;  
908 that is, a differential equation equates the rate of change in storage within a control volume with the  
909 difference between what comes in and what goes out of the control volume. In land surface modelling,  
910 for example, conservation laws are built into mechanistic models to ensure water and energy balance is  
911 preserved in simulations over time. ML models, however, do not automatically account for such laws and,  
912 as a result, water or energy can be *falsely* introduced or lost in the course of simulation.

913 **Monotonicity and rates:** The knowledge base includes the general characteristics of some causal  
914 relationships between various physical variables. For example, we know from basic thermodynamics that  
915 the relationship between melt rate and available heat is *monotonic*; that is, more heat causes a higher  
916 melt rate. Furthermore, we have some rough estimate of the feasible range of the *rate* of change in one  
917 with respect to the other. Similarly, from basic hydrology we know the causal relationships governing the  
918 way a hillslope stores and releases water are generally such that a positive correlation exists between  
919 water available in the soil and its contribution to flows; more water means more flows due to gravitational  
920 forces.

921 Mechanistic models directly account for such knowledge on casual relationships. This knowledge is  
922 encoded in process parametrizations typically in the form of deterministic, monotonic functions, or rarely  
923 in hysteretic forms, with a limited number of parameters to be calibrated to the specific case study in

924 hand (Gharari and Razavi, 2018). However, in the case of hyper-flexible models such as ANNs, such  
925 functions need to be entirely derived from data, all from scratch, and ignoring the knowledge base related  
926 to those monotonic relationships. Therefore, extrapolation runs the risk that such relationships become  
927 non-monotonic and/or have unrealistic rates, producing erroneous behaviors. This risk is exacerbated by  
928 the fact that identifying and diagnosing such errors are very difficult, if possible at all.

929 **Feedback mechanisms:** A real-world physical system is a combination of variables that interact over time,  
930 typically via a range of feedback mechanisms. Such feedback mechanisms control the internal dynamics  
931 of the system and are key to its evolution over time. For example, consider a coupled water-vegetation  
932 system in which precipitation, available soil moisture, and plant biomass interact in complex time-  
933 dependent ways, even at times creating positive feedbacks that destabilize the system's behavior  
934 (Rodriguez-Iturbe et al., 1991; Scheffer et al., 2001). The knowledge base available about these feedback  
935 mechanisms is often built into mechanistic models, using differential equations (ordinary or partial) to  
936 describe the system dynamics. The representation of such dynamics in the making of models is important,  
937 particularly for long-term predictions and over long time scales.

938 DL models are often unable to account explicitly for such long-term dynamics. If a particular dynamical  
939 behavior is present in training data, then DL can capture that behavior in its mapping from input onto  
940 output. DL however has no explicit mechanism to represent that dynamic under perturbed conditions  
941 beyond what has been recorded in the training data.

942 Is mechanistic modelling immune to issues with extrapolation? Certainly not. While a discussion on the  
943 limitations and prospects of mechanistic modelling is beyond this paper, one solution to improve  
944 extrapolability of mechanistic modelling over time that is also relevant to ML is 'space-for-time  
945 substitution'. This strategy is to investigate multiple or many sites simultaneously, instead of one, to infer  
946 a temporal trend for a site based on information from other sites that have different properties and/or  
947 experienced different conditions, assuming spatial and temporal variations are equivalent. For example,  
948 refer to Pickett (1989) and Blois et al. (2013) in the context of ecology and to Singh et al. (2011) in the  
949 context of hydrology. In the era of big data, ML can benefit significantly, explicitly or implicitly, from such  
950 strategies when spatio-temporal data across large domains are available. For example, Kratzert et al.  
951 (2019), Feng et al. (2020), and Ma et al. (2021) utilize the CAMELS dataset, which includes catchment  
952 attributes and hydrometeorological data across many different sites (Newman et al., 2014; Addor et al.,  
953 2017), to improve the performance of DL in hydrological modelling applications.

954 The bottom line is that mechanistic models are generally expected to be less prone to generating spurious  
955 behaviors in true out-of-sample prediction. Therefore, many domain experts may be inclined to trust  
956 physically based models as their behavior is constrained by physical laws that are perceived as unchanging  
957 with time. The points made in this section will become clearer in the next section, where the essential  
958 differences between DL and mechanistic modelling are discussed.

## 959 **8.2. Why is DL essentially different from process-based modelling?**

960 In the author's view, the first principles of ANNs are rooted in *connectionism*, *hyper-flexibility*, and  
961 *vigorous optimization*. These characteristics are fundamentally different from the guiding principles of  
962 developing and calibrating mechanistic models, as described in the following:

- 963 • *Connectionism* is an approach that orchestrates a set of simple algebraic operations in a massively  
964 parallel manner to create a model that is able to carry out complicated tasks. Following this  
965 approach, ANNs represent the response of a system under consideration to an input by summing  
966 the collective efforts of many neurons, whose roles cannot be easily attributed to individual  
967 processes involved in that system. This is unlike mechanistic modelling where each part of a model  
968 is designed to be responsible for a specific process.
- 969 • *Hyper-flexibility* is a characteristic of a model with excessive degrees of freedom, which can literally  
970 fit any dataset, and is not constrained by the many assumptions held by typical statistical models.  
971 ANNs are known to be hyper-flexible. Mechanistic models, however, have limited degrees of  
972 freedom depending on the knowledge base available about the processes being modelled. Ideally,  
973 mechanistic models tend to have just as many degrees of freedom as can be supported and  
974 constrained by available knowledge and data.
- 975 • *Vigorous optimization* here refers to the practice of manipulating model parameters at any cost to  
976 maximize the goodness-of-fit to calibration data. The training of ANNs is all about minimizing an error  
977 function; that is, among two competing ANNs, the one producing smaller errors in calibration and  
978 validation is the winner. Optimization is also often an essential part of mechanistic modelling to  
979 calibrate model parameters. However, in mechanistic modelling, minimizing the errors is not the  
980 goal but a means to improve the realism of the model. In other words, unlike ANNs, physical  
981 feasibility of a parameter, its identifiability, and equifinality are key considerations in mechanistic  
982 modelling.

983 The recognition of these fundamental differences is critically important when one aims to choose the right  
984 modelling paradigm for a purpose, compare the two paradigms in a case study, or attempt to bridge the  
985 two paradigms, possibly for improved modelling performance. The following section outlines the status  
986 quo for bridging the two paradigms and some emerging trends.

### 987 **8.3. How can we bridge DL and process-based modelling?**

988 The history of research on reconciling and bridging ANNs with mechanistic modelling dates back to the  
989 early 2000s or perhaps earlier. These efforts have generally had the objective of simultaneously leveraging  
990 the strengths of the two modelling paradigms to further our knowledge and predictive ability. **Abraham**  
991 **et al. (2012)** reviewed such research in the context of hydrology and refer to it as ‘hybridization’. They  
992 introduced three possible approaches for this purpose, which herein are referred to as ‘surrogate  
993 modelling’, ‘one-way coupling’, and ‘modular coupling’. Seven years later, **Reichstein et al. (2019)** in an  
994 influential article in *Nature* re-introduced and proposed the notion of ‘hybrid modelling’ and the above  
995 three approaches as the next steps in earth science. In the following, these three approaches are  
996 explained, and then more modern existing approaches arising from research fields beyond earth and  
997 environmental sciences are discussed.

998 **Surrogate modelling**, alternatively called metamodeling or model emulation, refers to the process of  
999 developing and applying a simpler, cheap-to-run model in lieu of a more complex, computationally  
1000 intensive model (**Razavi et al., 2012a**). In this process, a data-driven surrogate, such as an ANN, is trained  
1001 on samples of a limited number of original model runs to approximate the model response surface. The  
1002 developed surrogate model can then be used in different frameworks in conjunction with the original  
1003 model, as reviewed in **Razavi et al. (2012a)**, in multi-query applications such as optimization and

1004 uncertainty quantification. Example applications of ANNs as surrogates of mechanistic models include  
1005 [Johnson and Rogers \(2000\)](#), [Broad et al. \(2005\)](#), [Behzadian et al. \(2009\)](#), and [Vali et al. \(2020\)](#).

1006 **One-way coupling** refers to the process combining a mechanistic model with an ML model such that the  
1007 output of the former feeds into the latter as input. A general rationale for such a combination is that a  
1008 mechanistic model may not be able to fully explain the observed data and, therefore, an ML model could  
1009 be of help in extracting any information left in the residuals of the mechanistic model. For example,  
1010 consider a case where a mechanistic hydrologic model is used for streamflow forecasting and, as  
1011 expected, some errors in model outputs are present. An ANN can be used to model such errors over a  
1012 historical period to provide some predictive ability on the errors for a time step into the future. Then,  
1013 running these two models in sequence may provide higher forecasting skills. Example applications of such  
1014 one-way coupling include [Shamseldin and O'Connor \(2001\)](#) and [Ancil et al. \(2003\)](#), and [Li et al. \(in review\)](#).

1015 **Modular coupling** refers to cases where an ML model is used as a module/sub-model of a larger  
1016 mechanistic model or *vice versa*. The rationale for this type of coupling may be that a particular model  
1017 might have proven skills in representing a particular process and is therefore preferred, while other  
1018 processes are better represented by another model. Hydrologic examples are the work of [Chen and](#)  
1019 [Adams \(2006\)](#) and [Corzo et al. \(2009\)](#), in which ANNs are used as the routing module within a distributed  
1020 hydrological model. Another example is the work of [Chua and Wong \(2010\)](#) in which an ANN-based  
1021 hydrologic model takes the output of a kinematic wave model as one of its inputs. And, a recent example  
1022 is the work of [Bennett and Nijssen \(2020\)](#), in which a DL-based model for the simulation of turbulent heat  
1023 fluxes is built into a process-based hydrologic model.

1024 Beyond the earth and environmental sciences community, the notion of bridging the knowledge base and  
1025 ML has a long history (e.g., see the ‘knowledge-based artificial neural networks’ by [Towell and Shavlik](#)  
1026 [\(1994\)](#)), but it has received significantly more attention recently. Different approaches mostly arising from  
1027 mathematics and computer science have been proposed under titles such as ‘theory-guided data science’  
1028 [\(Karpatne et al., 2017\)](#), ‘informed machine learning’ [\(von Rueden et al., 2019\)](#), and ‘physics-informed  
1029 neural networks’ [\(Raissi et al., 2019\)](#), to name a few. Providing a full coverage of such approaches is well  
1030 beyond the scope of this paper, and many of them have been developed for specific application areas  
1031 with limited relevance to earth and environmental problems. Instead, in the following, I try to be selective  
1032 and explain three approaches that I found most relevant.

1033 **Regularizing ANNs via knowledge-based loss terms.** A new regularization function can be developed  
1034 based on the available knowledge surrounding a given problem and be added to the loss function used in  
1035 training. For example, any violation of the conservation laws or monotonicity of relationships, as described  
1036 in [Section 8.1](#), can be quantified and penalized during training. Refer to [Stewart and Ermon \(2017\)](#) for an  
1037 example application of this approach in the context of image processing.

1038 **Using mechanistic model runs to augment ANN training data.** A mechanistic model can be used to  
1039 simulate the system under investigation under a range of conditions to generate ‘synthetic data’ to  
1040 augment the available training data. This approach may be particularly useful in guiding ANNs in  
1041 extrapolation beyond conditions seen in the original training data (see the discussion in [Section 8.1](#)). This  
1042 approach is based on the assumption that the mechanistic model used is sufficiently accurate—an  
1043 assumption that needs to be treated with caution. For an example of this approach in the field of systems  
1044 biology, see [Deist et al. \(2019\)](#).

1045 **Integrating differential equations into ANNs.** This approach is a very recent and perhaps the most  
1046 mathematically elaborate in terms of integrating the knowledge base into ANNs, primarily developed by  
1047 [Raissi et al. \(2019\)](#). It parametrizes the known differential equations describing a system and integrates  
1048 them into the body of ANNs. The integrated model is then trained to the available data, simultaneously  
1049 inferring the parameters of the differential equations and network weights. One could view this approach  
1050 as an extension to the knowledge-based loss terms described above where the new loss term penalizes  
1051 the network for deviations from those known differential equations. This approach still seems embryonic  
1052 but perhaps with great potential for scientific breakthroughs.

#### 1053 **8.4. What can we learn from prominent DL applications?**

1054 As outlined in [Section 1](#), DL has already been used across a wide range of disciplines and applications with  
1055 varying degrees of success. Here, and for context, consider two special and well-known cases of DL  
1056 applications: playing chess and predicting the stock market. DL has achieved incredible, superhuman-level  
1057 performance in chess and similar games ([Silver et al., 2018](#)), while its performance in stock market  
1058 prediction has been criticized despite its widespread application (e.g., [Pearlstein, 2018](#)). These opposing  
1059 outcomes may be explained as follows:

- 1060 • Chess does not possess any properties of ‘complex systems’ ([Bar-Yam, 1997](#)), whereas financial  
1061 systems are essentially *complex*, with a wide range of agents interacting at a wide range of scales,  
1062 giving rise to emergent behaviors and even black swans. Any AI-based financial services themselves  
1063 would also be an agent influencing the stock market, even possibly inducing vicious cycles.
- 1064 • Chess can be viewed as a closed system, as no exogenous factors influence any properties or  
1065 dynamics of the board and players, whereas stock markets are open systems and, for any analyses,  
1066 the assumed boundary conditions depend on the analyst’s judgement.
- 1067 • Chess is a *fully observable* system, as the entire board, pieces, rules, and moves are seen by the  
1068 players, but stock markets are only *partially observable* and some controlling elements in the market  
1069 might be hidden to the analysts.
- 1070 • Chess is *stationary*, as the properties and governing rules of the game remain constant over time,  
1071 whereas stock markets are *non-stationary* and their long-term dynamics and behaviors may change  
1072 in unpredictable ways driven by political, social, economic, or natural events.

1073 So what? Earth and environmental systems arguably fall somewhere in between these two specific  
1074 applications with respect to their four fundamental and inter-related characteristics: such systems are  
1075 *complex, open, partially observable, and non-stationary*. Loosely speaking, understanding and predicting  
1076 earth and environmental systems face similar challenges to those of the stock markets in terms of those  
1077 four characteristics. However, unlike stock market systems that are conceived to be partially predictable  
1078 at best ([Fama, 1970](#); [Malkiel, 2003](#)), the behaviors of earth and environmental systems are generally  
1079 believed to be predictable, with limits of predictability that have been improving as more knowledge and  
1080 data become available.

1081 The comparisons above try to convey two points. First, the revolutionary success of DL in one field of  
1082 application cannot necessarily be extended directly to another field of application. The context matters,  
1083 and success depends on the characteristics of the problem at hand. Second, different disciplines may  
1084 cross-fertilize DL applications and learn from one another. However, cross-fertilization is non-trivial and

1085 requires more direct communications between experts in different disciplines about existing methods,  
1086 common issues, and ways forward.

## 1087 **9. Concluding remarks**

1088 Deep learning has perhaps by now served every researcher and practitioner in earth and environmental  
1089 sciences communities in tasks such as image and language processing, at least through their smart phones.  
1090 Such astonishing and within-reach technologies have boosted interest in DL, and in AI in general, within  
1091 these communities, evidenced by the significant growth in the number of their research papers on DL.  
1092 Many, including the author of this paper, believe the combination of AI with unprecedented data sources  
1093 and increased computational power will offer exciting new opportunities for expanding our knowledge  
1094 about various earth and environmental systems. Unsurprisingly, similar to many other innovations, AI and  
1095 particularly DL techniques are facing different views towards their future; for example, in the hydrology  
1096 context [Nearing et al. \(2020\)](#) suggest a DL-informed divorce from some of the current hydrological  
1097 theories while [Beven \(2020\)](#) advocates for the fundamental needs of a knowledge base in DL  
1098 interpretation.

1099 It is certainly an exciting time for earth and environmental sciences to benefit from DL tools. [Shen et al.](#)  
1100 [\(2018\)](#) picture a bright future but articulate some important technical and cultural challenges to overcome  
1101 in the years to come, by more targeted educational and organization efforts. We need also to be mindful  
1102 of any possible risk of hype and over-excitement about the new potential tools. Arguably, still many  
1103 applications of DL in earth and environmental sciences have primarily focused on off-the-shelf  
1104 applications of methods largely developed by mathematicians and computer scientists to problems in a  
1105 new domain with no or limited considerations of the available domain's knowledge base. The immediate  
1106 risk of such practices is that the popularity of AI tools in earth and environmental sciences would then  
1107 follow the ups and downs of these tools in the areas from which they originate and the software  
1108 developed for those purposes. There is also a greater risk, in the author's view, as follows.

1109 Let us flash back to more than three decades ago, when the prominent statistician [George Box \(1976, p.](#)  
1110 [797-798\)](#) warned about the “mathematistry” trap, “characterized by development of theory for theory's  
1111 sake, which since it seldom touches down with practice, has a tendency to redefine the problem rather  
1112 than solve it”. He argued that “there is unhappy evidence that mathematistry is not harmless. In such  
1113 areas as sociology, psychology, education, and even, I sadly say, engineering, investigators who are not  
1114 themselves statisticians sometimes take mathematistry seriously. Overawed by what they do not  
1115 understand, they mistakenly distrust their own common sense and adopt inappropriate procedures  
1116 devised by mathematicians with no scientific experience.” This sentiment was then echoed by the  
1117 prominent hydrologist [Vit Klemeš \(1986b, p. 177 and p. 185\)](#), who said “The danger increases with the  
1118 proliferation of computerized “hydrologic” models whose cheaply arranged ability to fit data is presented  
1119 as proof of their soundness and as a justification for using them for user-attractive but hydrologically  
1120 indefensible extrapolations.” He continued, “The danger to hydrology from extrapolations based on  
1121 mathematistry is that they lead it on the path of bad science.”

1122 The point here is that the risk of mathematistry seems to be just as fresh as it must have been back then,  
1123 particularly when it comes to the application of AI tools in earth and environmental sciences. Due to the  
1124 very nature of such tools, this risk may even well extend to their original areas of application, partly  
1125 because of their lack of explainability and interpretability ([see Rudin, 2019](#)), to a point that such practice

1126 has been referred to as a form of modern “alchemy”; see [Rahimi and Recht \(2017\)](#) for the sentiment,  
1127 [LeCun \(2017\)](#) for a rebuttal, and [Hutson \(2018\)](#) for a summary. This point is not to undermine the benefits  
1128 of AI technology, particularly for earth and environmental applications. Instead, it calls for improved rigor  
1129 and better appreciation of the knowledge base available. After all, it has been long known in  
1130 environmental sciences that complex models can be made to produce virtually any desired behavior given  
1131 their large degrees of freedom, as articulated by [Hornberger and Spear \(1981\)](#) three decades ago.

1132 Having such risks in mind, the new potential afforded by AI for earth and environmental sciences is great.  
1133 To realize this potential, we need to reconcile data-driven AI techniques and the theory-driven knowledge  
1134 base. The knowledge base is at the heart of ‘traditional programming’, which is still a major building block  
1135 of process-based or mechanistic modelling in earth and environmental sciences. Clearly, the traditional,  
1136 knowledge-based programming and AI are made up of two fundamentally different world views for  
1137 problem solving and, therefore, their reconciliation will not be straightforward. This paper tried to address  
1138 some critical questions in this regard and provide some perspective for this important endeavor, in  
1139 anticipation of new breakthroughs in earth and environmental sciences in an age of big data and  
1140 computational power.

## 1141 **Acknowledgements**

1142 The author is thankful for funding support from the Natural Sciences and Engineering Research Council of  
1143 Canada (Discovery Grants) and Integrated Modeling Program for Canada (IMPC) under the framework of  
1144 Global Water Futures (GWF).

## 1145 **References**

1146 Abbott, M.B., (1991). *Hydroinformatics: Information Technology and the Aquatic Environment*. Avebury  
1147 Technical. ISBN13 9781856288323.

1148 Abrahart, R. J., Anctil, F., Coulibaly, P., Dawson, C. W., Mount, N. J., See, L. M., ... & Wilby, R. L. (2012).  
1149 Two decades of anarchy? Emerging themes and outstanding challenges for neural network river  
1150 forecasting. *Progress in Physical Geography*, 36(4), 480-513.

1151 Addor, N., Newman, A. J., Mizukami, N., & Clark, M. P. (2017). The CAMELS data set: catchment attributes  
1152 and meteorology for large-sample studies. *Hydrology and Earth System Sciences*, 21(10), 5293-5313.

1153 Aizenberg, I., Aizenberg, N. N., & Vandewalle, J. P. L. (2000). *Multi-Valued and Universal Binary Neurons:  
1154 Theory, Learning and Applications*. Springer Science & Business Media.

1155 Anctil, F., Perrin, C., & Andréassian, V. (2003). ANN output updating of lumped conceptual rainfall/runoff  
1156 forecasting models, *Journal of the American Water Resources Association*, 39(5), 1269-1279.

1157 Ashouri, H., Hsu, K. L., Sorooshian, S., Braithwaite, D. K., Knapp, K. R., Cecil, L. D., ... & Prat, O. P. (2015).  
1158 PERSIANN-CDR: Daily precipitation climate data record from multisatellite observations for  
1159 hydrological and climate studies. *Bulletin of the American Meteorological Society*, 96(1), 69-83.

1160 Badran, F., Thiria, S., & Crepon, M. (1991). Wind ambiguity removal by the use of neural network  
1161 techniques. *Journal of Geophysical Research: Oceans*, 96(C11), 20521-20529.

- 1162 Bankert, R. L. (1994). Cloud classification of AVHRR imagery in maritime regions using a probabilistic neural  
1163 network. *Journal of Applied Meteorology*, 33(8), 909-918.
- 1164 Bar-Yam, Y. (1997). *Dynamics of Complex Systems*. Perseus Books, USA.
- 1165 Behzadian, K., Kapelan, Z., Savic, D., & Ardeshir, A. (2009). Stochastic sampling design using a multi-  
1166 objective genetic algorithm and adaptive neural networks. *Environmental Modelling & Software*,  
1167 24(4), 530-541.
- 1168 Benediktsson, J. A., Swain, P. H., & Ersoy, O. K. (1990). Neural network approaches versus statistical  
1169 methods in classification of multisource remote sensing data. *IEEE Transactions on Geoscience and*  
1170 *Remote Sensing*, 28(4).
- 1171 Bengio, Y., Simard, P., & Frasconi, P. (1994). Learning long-term dependencies with gradient descent is  
1172 difficult. *IEEE Transactions on Neural Networks*, 5(2), 157-166.
- 1173 Benítez, J. M., Castro, J. L., & Requena, I. (1997). Are artificial neural networks black boxes? *IEEE*  
1174 *Transactions on Neural Networks*, 8(5), 1156-1164.
- 1175 Bennett, A., & Nijssen, B. (2020). Deep learned process parameterizations provide better representations  
1176 of turbulent heat fluxes in hydrologic models. *Earth and Space Science Open Archive ESSOAr*.
- 1177 Bergen, K. J., Johnson, P. A., Maarten, V., & Beroza, G. C. (2019). Machine learning for data-driven  
1178 discovery in solid Earth geoscience. *Science*, 363(6433).
- 1179 Beven, K. (2020). Deep learning, hydrological processes and the uniqueness of place. *Hydrological*  
1180 *Processes*, 34, 3608–3613, <https://doi.org/10.1002/hyp.13805>.
- 1181 Beven, K. J. (2018). On hypothesis testing in hydrology: why falsification of models is still a really good  
1182 idea. *Wiley Interdisciplinary Reviews: Water*, 5(3), e1278.
- 1183 Beven, K., & Freer, J. (2001). Equifinality, data assimilation, and uncertainty estimation in mechanistic  
1184 modelling of complex environmental systems using the GLUE methodology. *Journal of Hydrology*,  
1185 249(1-4), 11-29.
- 1186 Blois, J. L., Williams, J. W., Fitzpatrick, M. C., Jackson, S. T., & Ferrier, S. (2013). Space can substitute for  
1187 time in predicting climate-change effects on biodiversity. *Proceedings of the National Academy of*  
1188 *Sciences*, 110(23), 9374-9379.
- 1189 Bottou, L. (1998). Online learning and stochastic approximations. *On-line learning in neural networks*,  
1190 17(9), 142.
- 1191 Bottou, L. (2010). Large-scale machine learning with stochastic gradient descent. In *Proceedings of*  
1192 *COMPSTAT'2010* (pp. 177-186). Physica-Verlag HD.
- 1193 Boursard, H., & Kamp, Y. (1988). Auto-association by multilayer perceptrons and singular value  
1194 decomposition. *Biological Cybernetics*, 59(4-5), 291-294.
- 1195 Box, G. E. (1976). Science and statistics. *Journal of the American Statistical Association*, 71(356), 791-799.

- 1196 Boznar, M., Lesjak, M., & Mlakar, P. (1993). A neural network-based method for short-term predictions of  
 1197 ambient SO<sub>2</sub> concentrations in highly polluted industrial areas of complex terrain. *Atmospheric*  
 1198 *Environment. Part B. Urban Atmosphere*, 27(2), 221-230.
- 1199 Broad, D. R., Dandy, G. C., & Maier, H. R. (2005). Water distribution system optimization using  
 1200 metamodels. *Journal of Water Resources Planning and Management*, 131(3), 172-180.
- 1201 Broomhead, D. S., & Lowe, D. (1988). Multivariable functional interpolation and adaptive networks.  
 1202 *Complex Systems*, 2, 321–355.
- 1203 Cabrera-Mercader, C. R., & Staelin, D. H. (1995). Passive microwave relative humidity retrievals using  
 1204 feedforward neural networks. *IEEE Transactions on Geoscience and Remote Sensing*, 33(6), 1324-  
 1205 1328.
- 1206 Castro, J. L., Mantas, C. J., & Benítez, J. M. (2002). Interpretation of artificial neural networks by means of  
 1207 fuzzy rules. *IEEE Transactions on Neural Networks*, 13(1), 101-116.
- 1208 Chen, J., & Adams, B. J. (2006). Integration of artificial neural networks with conceptual models in rainfall-  
 1209 runoff modeling. *Journal of Hydrology*, 318(1-4), 232-249.
- 1210 Cherkassky, V., & Ma, Y. Q. (2004). Practical selection of SVM parameters and noise estimation for SVM  
 1211 regression. *Neural Networks*, 17(1), 113–126.
- 1212 Chua, L. H., & Wong, T. S. (2010). Improving event-based rainfall–runoff modeling using a combined  
 1213 artificial neural network–kinematic wave approach. *Journal of Hydrology*, 390(1-2), 92-107.
- 1214 Corzo, G. A., Solomatine, D. P., Hidayat, de Wit, M., Werner, M., Uhlenbrook, S., and Price, R. K. (2009).  
 1215 Combining semi-distributed process-based and data-driven models in flow simulation: a case study  
 1216 of the Meuse river basin. *Hydrology and Earth System Sciences*, 13, 1619-1634,  
 1217 <https://doi.org/10.5194/hess-13-1619-2009>.
- 1218 Dangeti, P. (2017). *Statistics for Machine Learning*. Packt Publishing Ltd.
- 1219 de Villiers, J., and Barnard, E. (1993). Backpropagation neural nets with one and two hidden layers. *IEEE*  
 1220 *Transactions on Neural Networks*, 4(1), 136-141.
- 1221 DeBeer, C. M., Wheeler, H. S., Pomeroy, J. W., Barr, A. G., Baltzer, J. L., Johnstone, J. F., Turetsky, M. R.,  
 1222 Stewart, R. E., Hayashi, M., van der Kamp, G., Marshall, S., Campbell, E., Marsh, P., Carey, S. K.,  
 1223 Quinton, W. L., Li, Y., Razavi, S., Berg, A., McDonnell, J. J., Spence, C., Helgason, W. D., Ireson, A. M.,  
 1224 Black, T. A., Davison, B., Howard, A., Thériault, J. M., Shook, K., and Pietroniro, A. (2021). Summary  
 1225 and synthesis of Changing Cold Regions Network (CCRN) research in the interior of western Canada  
 1226 – Part 2: Future change in cryosphere, vegetation, and hydrology. *Hydrology and Earth System*  
 1227 *Sciences*, 25(4), 1849-1882.
- 1228 Dechter, R. (1986). *Learning while searching in constraint-satisfaction problems*. University of California,  
 1229 Computer Science Department, Cognitive Systems Laboratory.
- 1230 Deist, T. M., Patti, A., Wang, Z., Krane, D., Sorenson, T., & Craft, D. (2019). Simulation-assisted machine  
 1231 learning. *Bioinformatics*, 35(20), 4072-4080.

- 1232 Dengiz, B., Alabas-Uslu, C., & Dengiz, O. (2009). A tabu search algorithm for the training of neural  
1233 networks. *Journal of the Operational Research Society*, 60(2), 282-291.
- 1234 Devlin, J., Chang, M. W., Lee, K., & Toutanova, K. (2018). Bert: Pre-training of deep bidirectional  
1235 transformers for language understanding. arXiv preprint arXiv:1810.04805.
- 1236 Ducournau, A., & Fablet, R. (2016, December). Deep learning for ocean remote sensing: an application of  
1237 convolutional neural networks for super-resolution on satellite-derived SST data. In 2016 9th IAPR  
1238 Workshop on Pattern Recognition in Remote Sensing (PRRS) (pp. 1-6). IEEE.
- 1239 Duerr, O., Sick, B. and Murina, E., (2020), *Probabilistic Deep Learning: With Python, Keras and TensorFlow*  
1240 *Probability*, Publisher: Simon and Schuster, 296 pages, ISBN: 1617296074, 9781617296079 (available  
1241 online at: [https://livebook.manning.com/book/probabilistic-deep-learning-with-python/chapter-](https://livebook.manning.com/book/probabilistic-deep-learning-with-python/chapter-1/72)  
1242 [1/72](https://livebook.manning.com/book/probabilistic-deep-learning-with-python/chapter-1/72))
- 1243 Elman, J. L. (1990). Finding structure in time. *Cognitive Science*, 14(2), 179-211.
- 1244 Eyring, V., Bony, S., Meehl, G. A., Senior, C. A., Stevens, B., Stouffer, R. J., & Taylor, K. E. (2016). Overview  
1245 of the Coupled Model Intercomparison Project Phase 6 (CMIP6) experimental design and  
1246 organization. *Geoscientific Model Development*, 9(5), 1937-1958.
- 1247 Fama, E. F. (1970). Efficient capital markets: a review of theory and empirical work. *The Journal of Finance*,  
1248 25(2), 383-417.
- 1249 Fang, X., & Pomeroy, J. W. (2020). Diagnosis of future changes in hydrology for a Canadian Rockies  
1250 headwater basin. *Hydrology and Earth System Sciences*, 24(5), 2731-2754.
- 1251 Feng, D., Fang, K., & Shen, C. (2020). Enhancing streamflow forecast and extracting insights using long-  
1252 short term memory networks with data integration at continental scales. *Water Resources Research*,  
1253 56(9), e2019WR026793.
- 1254 Foresee, F. D., & Hagan, M. T. (1997, June). Gauss-Newton approximation to Bayesian learning. In  
1255 *Proceedings of International Conference on Neural Networks (ICNN'97)* (Vol. 3, pp. 1930-1935). IEEE.
- 1256 Frasconi, P., Gori, M., & Soda, G. (1992). Local feedback multilayered networks. *Neural Computation*, 4(1),  
1257 120-130.
- 1258 Friedman, J. H. (1991). Multivariate adaptive regression splines. *Annals of Statistics*, 19(1), 1–67.
- 1259 Gardner, M. W., & Dorling, S. R. (1998). Artificial neural networks (the multilayer perceptron)—a review  
1260 of applications in the atmospheric sciences. *Atmospheric Environment*, 32(14-15), 2627-2636.
- 1261 Gelaro, R., McCarty, W., Suárez, M. J., Todling, R., Molod, A., Takacs, L., ... & Wargan, K. (2017). The  
1262 modern-era retrospective analysis for research and applications, version 2 (MERRA-2). *Journal of*  
1263 *Climate*, 30(14), 5419-5454.
- 1264 Gharari, S., & Razavi, S. (2018). A review and synthesis of hysteresis in hydrology and hydrological  
1265 modeling: memory, path-dependency, or missing physics? *Journal of Hydrology*, 566, 500-519.
- 1266 Glorot, X., Bordes, A., & Bengio, Y. (2011, June). Deep sparse rectifier neural networks. In *Proceedings of*  
1267 *the 14<sup>th</sup> International Conference on Artificial Intelligence and Statistics* (pp. 315-323).

- 1268 Goodfellow, I., Bengio, Y., Courville, A., & Bengio, Y. (2016). Deep learning (Vol. 1). Cambridge: MIT Press.
- 1269 Goodfellow, I., Pouget-Abadie, J., Mirza, M., Xu, B., Warde-Farley, D., Ozair, S., Courville, A., and Bengio,  
1270 Y. (2014). Generative adversarial networks. Proceedings of the International Conference on Neural  
1271 Information Processing Systems (NIPS 2014). pp. 2672–2680.
- 1272 Gu, H., Xu, Y. P., Ma, D., Xie, J., Liu, L., & Bai, Z. (2020). A surrogate model for the Variable Infiltration  
1273 Capacity model using deep learning artificial neural network. *Journal of Hydrology*, 588, 125019.
- 1274 Guillaume, J. H., Jakeman, J. D., Marsili-Libelli, S., Asher, M., Brunner, P., Croke, B., ... & Stigter, J. D. (2019).  
1275 Introductory overview of identifiability analysis: a guide to evaluating whether you have the right  
1276 type of data for your modeling purpose. *Environmental Modelling & Software*, 119, 418-432.
- 1277 Gupta, H. V., Clark, M. P., Vrugt, J. A., Abramowitz, G., & Ye, M. (2012). Towards a comprehensive  
1278 assessment of model structural adequacy. *Water Resources Research*, 48(8).
- 1279 Hagan, M. T., & Menhaj, M. B. (1994). Training feedforward networks with the Marquardt algorithm. *IEEE*  
1280 *Transactions on Neural Networks*, 5(6), 989-993.
- 1281 Hagan, M. T., Demuth, H. B., & Beale, M. (1996). *Neural network design*. PWS Publishing Company, Boston,  
1282 MA.
- 1283 Hendler, J. (2008). Avoiding another AI winter. *IEEE Intelligent Systems*, (2), 2-4.
- 1284 Hinton, G. E., McClelland, J., & Rumelhart, D. (1986). Distributed representations. In D. E. Rumelhart & J.  
1285 L. McClelland, editors, *Parallel Distributed Processing: Explorations in the Microstructure of*  
1286 *Cognition*, volume 1, pages 77–109. MIT Press, Cambridge.
- 1287 Hinton, G. E., Osindero, S., & Teh, Y. W. (2006). A fast learning algorithm for deep belief nets. *Neural*  
1288 *Computation*, 18(7), 1527-1554.
- 1289 Hinton, G. E., Srivastava, N., Krizhevsky, A., Sutskever, I., & Salakhutdinov, R. R. (2012). Improving neural  
1290 networks by preventing co-adaptation of feature detectors. arXiv preprint arXiv:1207.0580.
- 1291 Hochreiter, S., & Schmidhuber, J. (1997). Long short-term memory. *Neural Computation*, 9(8), 1735-1780.
- 1292 Hornberger, G. M., & Spear, R. C. (1981). Approach to the preliminary analysis of environmental systems.  
1293 *J. Environ. Mgmt.*, 12(1), 7-18.
- 1294 Hornik, K., Stinchcombe, M., & White, H. (1989). Multilayer feedforward networks are universal  
1295 approximators. *Neural Networks*, 2(5), 359-366.
- 1296 Hosny, A., Parmar, C., Quackenbush, J., Schwartz, L. H., & Aerts, H. J. (2018). Artificial intelligence in  
1297 radiology. *Nature Reviews Cancer*, 18(8), 500-510.
- 1298 Hsu, K. L., Gao, X., Sorooshian, S., & Gupta, H. V. (1997). Precipitation estimation from remotely sensed  
1299 information using artificial neural networks. *Journal of Applied Meteorology*, 36(9), 1176-1190.
- 1300 Hsu, K. L., Gupta, H. V., & Sorooshian, S. (1995). Artificial neural network modeling of the rainfall-runoff  
1301 process. *Water Resources Research*, 31(10), 2517-2530.

- 1302 Hutson, M. (2018). Has artificial intelligence become alchemy? *Science*, 360(6388), 478. DOI:  
1303 10.1126/science.360.6388.478
- 1304 Johansen, T. A. (1997). On Tikhonov regularization, bias and variance in nonlinear system identification.  
1305 *Automatica*, 33(3), 441-446.
- 1306 Johnson, V. M., & Rogers, L. L. (2000). Accuracy of neural network approximators in simulation-  
1307 optimization. *Journal of Water Resources Planning and Management*, 126(2), 48-56.
- 1308 Jordan, M. I. (1986). Attractor dynamics and parallelism in a connectionist sequential machine. In 8th  
1309 Annual Conference, Cognitive Science Society. MIT Press: Amherst, MA; 531–546.
- 1310 Jordan, M. I., & Mitchell, T. M. (2015). Machine learning: trends, perspectives, and prospects. *Science*,  
1311 349(6245), 255-260.
- 1312 Kang, K. W., Park, C. Y., & Kim, J. H. (1993). Neural network and its application to rainfall-runoff forecasting.  
1313 *Korean Journal of Hydrosiences*, 4, 1-9.
- 1314 Karamouz, M., Razavi, S., & Araghinejad, S. (2008). Long-lead seasonal rainfall forecasting using time-delay  
1315 recurrent neural networks: a case study. *Hydrological Processes: An International Journal*, 22(2), 229-  
1316 241.
- 1317 Karpatne, A., Atluri, G., Faghmous, J. H., Steinbach, M., Banerjee, A., Ganguly, A., ... & Kumar, V. (2017).  
1318 Theory-guided data science: a new paradigm for scientific discovery from data. *IEEE Transactions on*  
1319 *Knowledge and Data Engineering*, 29(10), 2318-2331.
- 1320 Kennedy, M. C., & O'Hagan, A. (2000). Predicting the output from a complex computer code when fast  
1321 approximations are available. *Biometrika*, 87(1), 1–13.
- 1322 Khatami, S., Peel, M. C., Peterson, T. J., & Western, A. W. (2019). Equifinality and flux mapping: A new  
1323 approach to model evaluation and process representation under uncertainty. *Water Resources*  
1324 *Research*, 55(11), 8922-8941.
- 1325 Kim, S. S. (1998). Time-delay recurrent neural network for temporal correlations and prediction.  
1326 *Neurocomputing*, 20(1-3), 253-263.
- 1327 Kirchner, J. W. (2006). Getting the right answers for the right reasons: linking measurements, analyses,  
1328 and models to advance the science of hydrology. *Water Resources Research*, 42(3).
- 1329 Klemeš, V. (1986a). Operational testing of hydrological simulation models. *Hydrological Sciences Journal*,  
1330 31(1), 13-24.
- 1331 Klemeš, V. (1986b). Dilettantism in hydrology: transition or destiny? *Water Resources Research*, 22(9S),  
1332 177S-188S.
- 1333 Kolakowski, M. (2018). How Algo Trading Is Worsening Stock Market Routs, Investopedia  
1334 (<https://www.investopedia.com/news/how-algo-trading-worsening-stock-market-routs/>)
- 1335 Krasnopolsky, V. M. (2007). Neural network emulations for complex multidimensional geophysical  
1336 mappings: applications of neural network techniques to atmospheric and oceanic satellite retrievals  
1337 and numerical modeling. *Reviews of Geophysics*, 45(3).

- 1338 Kratzert, F., Klotz, D., Brenner, C., Schulz, K., & Herrnegger, M. (2018). Rainfall–runoff modelling using long  
1339 short-term memory (LSTM) networks. *Hydrology and Earth System Sciences*, 22(11), 6005-6022.
- 1340 Kratzert, F., Klotz, D., Herrnegger, M., Sampson, A. K., Hochreiter, S., & Nearing, G. S. (2019). Toward  
1341 improved predictions in ungauged basins: Exploiting the power of machine learning. *Water*  
1342 *Resources Research*, 55(12), 11344-11354.
- 1343 Krizhevsky, A., Sutskever, I., & Hinton, G. E. (2017). Imagenet classification with deep convolutional neural  
1344 networks. *Communications of the ACM*, 60(6), 84-90.
- 1345 Krogh, A., & Hertz, J. (1991). A simple weight decay can improve generalization. *Advances in Neural*  
1346 *Information Processing Systems*, 4, 950-957.
- 1347 Lawrence, S., Giles, C. L., Tsoi, A. C., & Back, A. D. (1997). Face recognition: a convolutional neural-network  
1348 approach. *IEEE Transactions on Neural Networks*, 8(1), 98-113.
- 1349 LeCun, Y. (2017). My take on Ali Rahimi's "Test of Time" award talk at NIPS, (accessed online in December  
1350 2020 at: [https://www2.isye.gatech.edu/~tzhao80/Yann\\_Response.pdf](https://www2.isye.gatech.edu/~tzhao80/Yann_Response.pdf))
- 1351 Lee, J., Kim, R., Koh, Y., & Kang, J. (2019). Global stock market prediction based on stock chart images  
1352 using deep Q-network. *IEEE Access*, 7, 167260-167277.
- 1353 Li, D., Marshall, L., Liang, Z., Sharma, A., and Zhou, Y. (in review), Characterizing distributed hydrological  
1354 model residual errors using a probabilistic Long Short-Term Memory network, *Journal of Hydrology*
- 1355 Lindström, G., Johansson, B., Persson, M., Gardelin, M., & Bergström, S. (1997). Development and test of  
1356 the distributed HBV-96 hydrological model. *Journal of hydrology*, 201(1-4), 272-288.
- 1357 Ma, K., Feng, D., Lawson, K., Tsai, W. P., Liang, C., Huang, X., ... & Shen, C. (2021). Transferring Hydrologic  
1358 Data Across Continents–Leveraging Data-Rich Regions to Improve Hydrologic Prediction in Data-  
1359 Sparse Regions. *Water Resources Research*, 57(5), e2020WR028600.
- 1360 MacKay, D. J. (1992). A practical Bayesian framework for backpropagation networks. *Neural Computation*,  
1361 4(3), 448-472.
- 1362 Maier, H. R., & Dandy, G. C. (2000). Neural networks for the prediction and forecasting of water resources  
1363 variables: a review of modelling issues and applications. *Environmental Modelling & Software*, 15(1),  
1364 101-124.
- 1365 Maier, H. R., Jain, A., Dandy, G. C., & Sudheer, K. P. (2010). Methods used for the development of neural  
1366 networks for the prediction of water resource variables in river systems: current status and future  
1367 directions. *Environmental Modelling & Software*, 25(8), 891-909.
- 1368 Malkiel, B. G. (2003). The efficient market hypothesis and its critics. *Journal of Economic Perspectives*,  
1369 17(1), 59-82.
- 1370 McCann, D. W. (1992). A neural network short-term forecast of significant thunderstorms. *Weather and*  
1371 *Forecasting*, 7(3), 525-534.
- 1372 Milly, P. C. D., Betancourt, J., Falkenmark, M., Hirsch, R. M., Kundzewicz, Z. W., Lettenmaier, D. P., &  
1373 Stouffer, R. J. (2008). Stationarity is dead: whither water management? *Science*, 319, 573-574.

- 1374 Minns, A. W., & Hall, M. J. (1996). Artificial neural networks as rainfall-runoff models. *Hydrological*  
1375 *Sciences Journal*, 41(3), 399-417.
- 1376 Minsky, M., & Papert, S. A. (1969). *Perceptrons: An Introduction to Computational Geometry*. MIT Press.
- 1377 Nash, J. E., & Sutcliffe, J. V. (1970). River flow forecasting through conceptual models part I—A discussion  
1378 of principles. *Journal of Hydrology*, 10(3), 282-290.
- 1379 Navone, H. D., & Ceccatto, H. A. (1994). Predicting Indian monsoon rainfall: a neural network approach.  
1380 *Climate Dynamics*, 10(6-7), 305-312.
- 1381 Nearing, G. S., Kratzert, F., Sampson, A. K., Pelissier, C. S., Klotz, D., Frame, J. M., ... & Gupta, H. V. (2020).  
1382 What role does hydrological science play in the age of machine learning?. *Water Resources Research*,  
1383 e2020WR028091.
- 1384 Newman, A. Sampson, K., Clark, M. P., Bock, A. Viger, R. J., Blodgett, D., (2014). A large-sample watershed-  
1385 scale hydrometeorological dataset for the contiguous USA. Boulder, CO: UCAR/NCAR.  
1386 <https://dx.doi.org/10.5065/D6MW2F4D>
- 1387 Oreskes, N., Shrader-Frechette, K., & Belitz, K. (1994). Verification, validation, and confirmation of  
1388 numerical models in the earth sciences. *Science*, 263(5147), 641-646.
- 1389 Pan, B., Hsu, K., AghaKouchak, A., & Sorooshian, S. (2019). Improving precipitation estimation using  
1390 convolutional neural network. *Water Resources Research*, 55(3), 2301-2321.
- 1391 Panchal, J. H., Fuge, M., Liu, Y., Missoum, S., & Tucker, C. (2019). Machine learning for engineering design.  
1392 *Journal of Mechanical Design*, 141(11).
- 1393 Pearlstein, S. (2018). The robots-vs.-robots trading that has hijacked the stock market, *The Washington*  
1394 *Post*, [https://www.washingtonpost.com/news/wonk/wp/2018/02/07/the-robots-v-robots-trading-  
1395 that-has-hijacked-the-stock-market/](https://www.washingtonpost.com/news/wonk/wp/2018/02/07/the-robots-v-robots-trading-that-has-hijacked-the-stock-market/)
- 1396 Pickett, S. T. (1989). Space-for-time substitution as an alternative to long-term studies. In *Long-term*  
1397 *studies in ecology* (pp. 110-135). Springer, New York, NY.
- 1398 Prechelt, L. (1998). Early stopping-but when? In G. Montavon, G. B. Orr, & K.-R. Müller, editors, *Neural*  
1399 *Networks: Tricks of the Trade*, pages 55-69. Springer, Berlin, Heidelberg.
- 1400 Rahimi, A., and & Recht, B., (2017)., Back when we were kids, Test-of-time award presentation,  
1401 *Conference on Neural Information Processing Systems, 2017, Vancouver, Canada* (Video online  
1402 accessed in December, 2020, at from: <https://youtu.be/Qi1Yry33TQE>).
- 1403 Raina, R., Madhavan, A., & Ng, A. Y. (2009, June). Large-scale deep unsupervised learning using graphics  
1404 processors. In *Proceedings of the 26th Annual International Conference on Machine Learning* (pp.  
1405 873-880).
- 1406 Raissi, M., Perdikaris, P., & Karniadakis, G. E. (2019). Physics-informed neural networks: a deep learning  
1407 framework for solving forward and inverse problems involving nonlinear partial differential  
1408 equations. *Journal of Computational Physics*, 378, 686-707.

- 1409 Rajbhandari, S., Rasley, J., Ruwase, O., & He, Y. (2019). ZeRO: memory optimization towards training a  
1410 trillion parameter models. arXiv preprint arXiv:1910.02054.
- 1411 Rakitianskaia, A., & Engelbrecht, A. P. (2009). Training neural networks with PSO in dynamic environments.  
1412 In 2009 IEEE Congress on Evolutionary Computation (pp. 667-673).
- 1413 Razavi, S., & Araghinejad, S. (2009). Reservoir inflow modeling using temporal neural networks with  
1414 forgetting factor approach. *Water Resources Management*, 23(1), 39-55.
- 1415 Razavi, S., & Karamouz, M. (2007). Adaptive neural networks for flood routing in river systems. *Water  
1416 international*, 32(3), 360-375.
- 1417 Razavi, S., & Tolson, B. A. (2011). A new formulation for feedforward neural networks. *IEEE Transactions  
1418 on Neural Networks*, 22(10), 1588-1598.
- 1419 Razavi, S., Elshorbagy, A., Wheeler, H., & Sauchyn, D. (2015). Toward understanding nonstationarity in  
1420 climate and hydrology through tree ring proxy records. *Water Resources Research*, 51(3), 1813-1830.
- 1421 Razavi, S., Jakeman, A., Saltelli, A., Prieur, C., Iooss, B., Borgonovo, E., ... & Tarantola, S. (2021). The future  
1422 of sensitivity analysis: an essential discipline for systems modeling and policy support.  
1423 *Environmental Modelling & Software*, 104954.
- 1424 Razavi, S., Sheikholeslami, R., Gupta, H. V., & Haghnegahdar, A. (2019). VARS-TOOL: A toolbox for  
1425 comprehensive, efficient, and robust sensitivity and uncertainty analysis. *Environmental Modelling  
1426 & Software*, 112, 95-107.
- 1427 Razavi, S., Tolson, B. A., & Burn, D. H. (2012a). Review of surrogate modeling in water resources. *Water  
1428 Resources Research*, 48(7).
- 1429 Razavi, S., Tolson, B. A., & Burn, D. H. (2012b). Numerical assessment of metamodelling strategies in  
1430 computationally intensive optimization. *Environmental Modelling & Software*, 34, 67-86.
- 1431 Reed, R. (1993). Pruning algorithms—A survey. *IEEE Transactions on Neural Networks*, 4(5), 740–747.
- 1432 Reichstein, M., Camps-Valls, G., Stevens, B., Jung, M., Denzler, J., & Carvalhais, N. (2019). Deep learning  
1433 and process understanding for data-driven Earth system science. *Nature*, 566(7743), 195-204.
- 1434 Rodriguez-Iturbe, I., Entekhabi, D., Lee, J. S., & Bras, R. L. (1991). Nonlinear dynamics of soil moisture at  
1435 climate scales: 2. Chaotic analysis. *Water Resources Research*, 27(8), 1907-1915.
- 1436 Rosenblatt, F. (1957). The perceptron, a perceiving and recognizing automaton (Project PARA), Cornell  
1437 Aeronautical Laboratory Report No. 85-460-1, Buffalo, New York.
- 1438 Rudin, C. (2019). Stop explaining black box machine learning models for high stakes decisions and use  
1439 interpretable models instead. *Nature Machine Intelligence*, 1(5), 206-215.
- 1440 Rumelhart, D. E., Hinton, G. E., & Williams, R. J. (1986). Learning representations by back-propagating  
1441 errors. *Nature*, 323(6088), 533-536.
- 1442 Samek, W., and Müller, K.-R. (2019). Towards Explainable Artificial Intelligence. In *Explainable AI:  
1443 Interpreting, Explaining and Visualizing Deep Learning* (pp. 5-22). doi:10.1007/978-3-030-28954-6\_1.

- 1444 Scheffer, M., Carpenter, S., Foley, J. A., Folke, C., & Walker, B. (2001). Catastrophic shifts in ecosystems.  
1445 Nature, 413(6856), 591-596.
- 1446 Schmidhuber, J. (2015a). "Deep Learning". Scholarpedia. 10(11), 32832. Bibcode:2015SchpJ..1032832S.  
1447 doi:10.4249/scholarpedia.32832.
- 1448 Schmidhuber, J. (2015b). Deep learning in neural networks: an overview. Neural Networks, 61, 85-117.
- 1449 See, L. M., Jain, A., Dawson, C.W., and Abrahart, R.J. (2008). Visualisation of Hidden Neuron Behaviour in  
1450 a Neural Network Rainfall-Runoff Model. In: Practical Hydroinformatics: Computational Intelligence  
1451 and Technological Developments in Water Applications (Abrahart, See, Solomatine, eds.). Springer,  
1452 pp 87-99.
- 1453 Shamseldin, A. Y., & O'Connor, K. M. (2001). A non-linear neural network technique for updating of river  
1454 flow forecasts. Hydrology and Earth System Sciences, 5, 577–598, [https://doi.org/10.5194/hess-5-](https://doi.org/10.5194/hess-5-577-2001)  
1455 [577-2001](https://doi.org/10.5194/hess-5-577-2001).
- 1456 Shen, C. (2018). A transdisciplinary review of deep learning research and its relevance for water resources  
1457 scientists. Water Resources Research, 54(11), 8558-8593.
- 1458 Shi, X., Chen, Z., Wang, H., Yeung, D. Y., Wong, W. K., & Woo, W. C. (2015). Convolutional LSTM network:  
1459 a machine learning approach for precipitation nowcasting. In Advances in Neural Information  
1460 Processing Systems (pp. 802-810).
- 1461 Shi, X., Gao, Z., Lausen, L., Wang, H., Yeung, D. Y., Wong, W. K., & Woo, W. C. (2017). Deep learning for  
1462 precipitation nowcasting: A benchmark and a new model. arXiv preprint arXiv:1706.03458.
- 1463 Silver, D., Hubert, T., Schrittwieser, J., Antonoglou, I., Lai, M., Guez, A., ... & Lillicrap, T. (2018). A general  
1464 reinforcement learning algorithm that masters chess, shogi, and Go through self-play. Science,  
1465 362(6419), 1140-1144.
- 1466 Singh, R., Wagener, T., Werkhoven, K. V., Mann, M. E., & Crane, R. (2011). A trading-space-for-time  
1467 approach to probabilistic continuous streamflow predictions in a changing climate—accounting for  
1468 changing watershed behavior. Hydrology and Earth System Sciences, 15(11), 3591-3603.
- 1469 Sorooshian, S., Hsu, K. L., Gao, X., Gupta, H. V., Imam, B., & Braithwaite, D. (2000). Evaluation of PERSIANN  
1470 system satellite-based estimates of tropical rainfall. Bulletin of the American Meteorological Society,  
1471 81(9), 2035-2046.
- 1472 Srivastava, N., Hinton, G., Krizhevsky, A., Sutskever, I., & Salakhutdinov, R. (2014). Dropout: a simple way  
1473 to prevent neural networks from overfitting. The Journal of Machine Learning Research, 15(1), 1929-  
1474 1958.
- 1475 Stewart, R., & Ermon, S. (2017, February). Label-free supervision of neural networks with physics and  
1476 domain knowledge. In 31<sup>st</sup> AAAI Conference on Artificial Intelligence.
- 1477 Stogryn, A. P., Butler, C. T., & Bartolac, T. J. (1994). Ocean surface wind retrievals from special sensor  
1478 microwave imager data with neural networks. Journal of Geophysical Research: Oceans, 99(C1), 981-  
1479 984.

- 1480 Tamura, S., & Tateishi, M. (1997). Capabilities of a four-layered feedforward neural network: four layers  
1481 versus three. *IEEE Transactions on Neural Networks*, 8(2), 251–255.
- 1482 Tang, G., Long, D., Behrangi, A., Wang, C., & Hong, Y. (2018). Exploring deep neural networks to retrieve  
1483 rain and snow in high latitudes using multisensor and reanalysis data. *Water Resources Research*,  
1484 54(10), 8253-8278.
- 1485 Tao, Y., Gao, X., Hsu, K., Sorooshian, S., & Ihler, A. (2016). A deep neural network modeling framework to  
1486 reduce bias in satellite precipitation products. *Journal of Hydrometeorology*, 17(3), 931-945.
- 1487 Tao, Y., Hsu, K., Ihler, A., Gao, X., & Sorooshian, S. (2018). A two-stage deep neural network framework  
1488 for precipitation estimation from bispectral satellite information. *Journal of Hydrometeorology*,  
1489 19(2), 393-408.
- 1490 Teoh, E. J., Tan, K. C., & Xiang, C. (2006). Estimating the number of hidden neurons in a feedforward  
1491 network using the singular value decomposition. *IEEE Transactions on Neural Networks*, 17(6), 1623-  
1492 1629.
- 1493 Tickle, A. B., Andrews, R., Golea, M., & Diederich, J. (1998). The truth will come to light: directions and  
1494 challenges in extracting the knowledge embedded within trained artificial neural networks. *IEEE*  
1495 *Transactions on Neural Networks*, 9(6), 1057-1068.
- 1496 Tikhonov, A. N. and V. Y. Arsenin (1977). *Solutions of Ill-posed Problems*. Winston, Washington DC, 258  
1497 pages.
- 1498 Tokar, A. S., & Markus, M. (2000). Precipitation-runoff modeling using artificial neural networks and  
1499 conceptual models. *Journal of Hydrologic Engineering*, 5(2), 156-161.
- 1500 Torresen, J. (2018). A review of future and ethical perspectives of robotics and AI. *Frontiers in Robotics*  
1501 *and AI*, 4, 75.
- 1502 Towell, G. G., & Shavlik, J. W. (1994). Knowledge-based artificial neural networks. *Artificial Intelligence*,  
1503 70(1-2), 119-165.
- 1504 Vali, M., Zare, M., & Razavi, S. (2020). Automatic clustering-based surrogate-assisted genetic algorithm  
1505 for groundwater remediation system design. *Journal of Hydrology*, 125752.
- 1506 Vapnik, V. (1998) *Statistical Learning Theory*, Wiley, New York.
- 1507 von Rueden, L., Mayer, S., Beckh, K., Georgiev, B., Giesselbach, S., Heese, R., ... & Walczak, M. (2019).  
1508 Informed machine learning—A taxonomy and survey of integrating knowledge into learning systems.  
1509 arXiv preprint arXiv:1903.12394.
- 1510 Waibel, A., Hanazawa, T., Hintin, G., Shikano, K., Lang, K. J. (1989). Phoneme recognition using time delay  
1511 neural networks. *IEEE Transactions on Acoustics, Speech, and Signal Processing*, 37(3), 328–339.
- 1512 Wexler, R. (2017). When a Computer Program Keeps You in Jail. *The New York Times*  
1513 ([https://www.nytimes.com/2017/06/13/opinion/how-computers-are-harming-criminal-  
1514 justice.html?auth=login-google](https://www.nytimes.com/2017/06/13/opinion/how-computers-are-harming-criminal-justice.html?auth=login-google))

- 1515 Wilby, R. L., Abrahart, R. J., & Dawson, C. W. (2003). Detection of conceptual model rainfall—runoff  
1516 processes inside an artificial neural network. *Hydrological Sciences Journal*, 48(2), 163-181.
- 1517 Xiang, C., Ding, S. Q., & Lee, T. H. (2005). Geometrical interpretation and architecture selection of MLP.  
1518 *IEEE Transactions on Neural Networks*, 16(1), 84-96.
- 1519 Xu, Y., Wong, K. W., & Leung, C. S. (2006). Generalized RLS approach to the training of neural networks.  
1520 *IEEE Transactions on Neural Networks*, 17(1), 19–34.
- 1521 Young, T., Hazarika, D., Poria, S., & Cambria, E. (2018). Recent trends in deep learning based natural  
1522 language processing. *IEEE Computational Intelligence Magazine*, 13(3), 55-75.
- 1523 Yu, X., Cui, T., Sreekanth, J., Mangeon, S., Doble, R., Xin, P., ... & Gilfedder, M. (2020). Deep learning  
1524 emulators for groundwater contaminant transport modelling. *Journal of Hydrology*, 590, 125351.